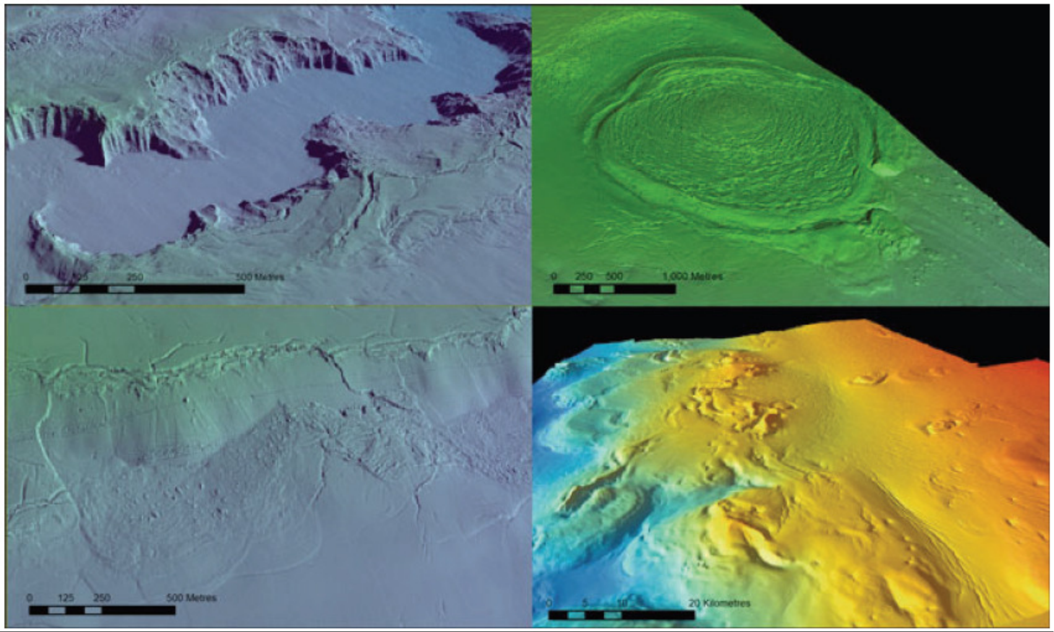

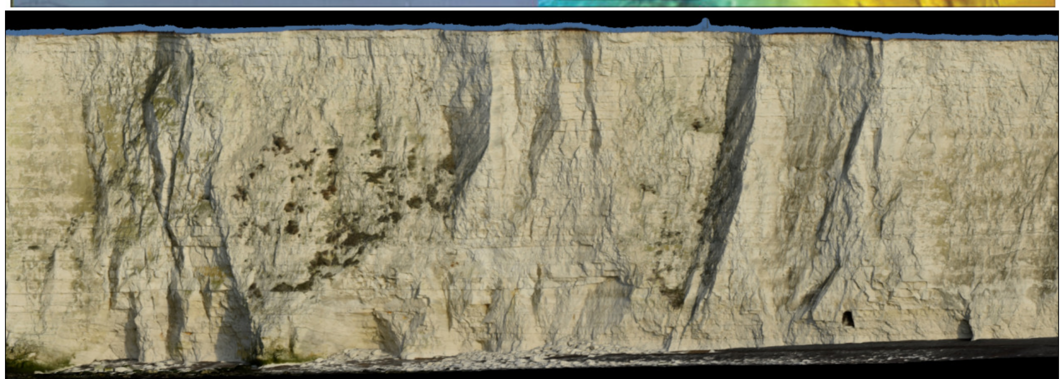

Use of LiDAR and photogrammetry to develop predictive models of slope stability

Oliver Dabson and Jamie Gilham

Tuesday, 15 October 2019

JACOBS

What is LiDAR?

- **Li**ght **D**etection **A**nd **R**anging
- A remote sensing method using pulsed laser to measure distances to the Earth
- Generates precise information about the shape of the Earth
- 2 types of LiDAR:
  - Topographic (NIR)
  - Bathymetric (green)

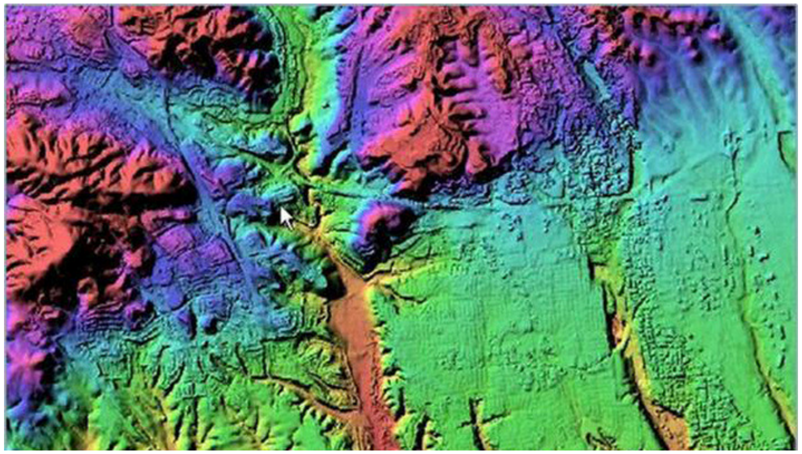

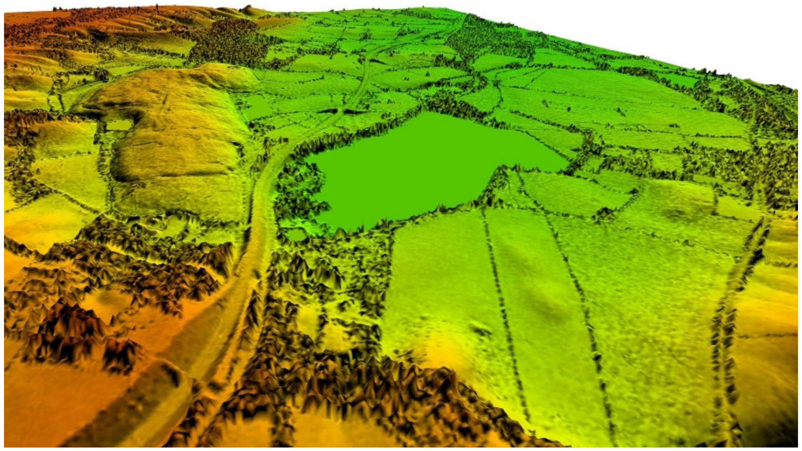

Image credit: BAE systems

LiDAR data collection

- Major hardware components:
  - Laser scanner system
  - GPS (global positioning system)
  - INS (inertial navigational system)
  - Collection vehicle
- Laser beam is transmitted towards target and the reflection is detected and analysed

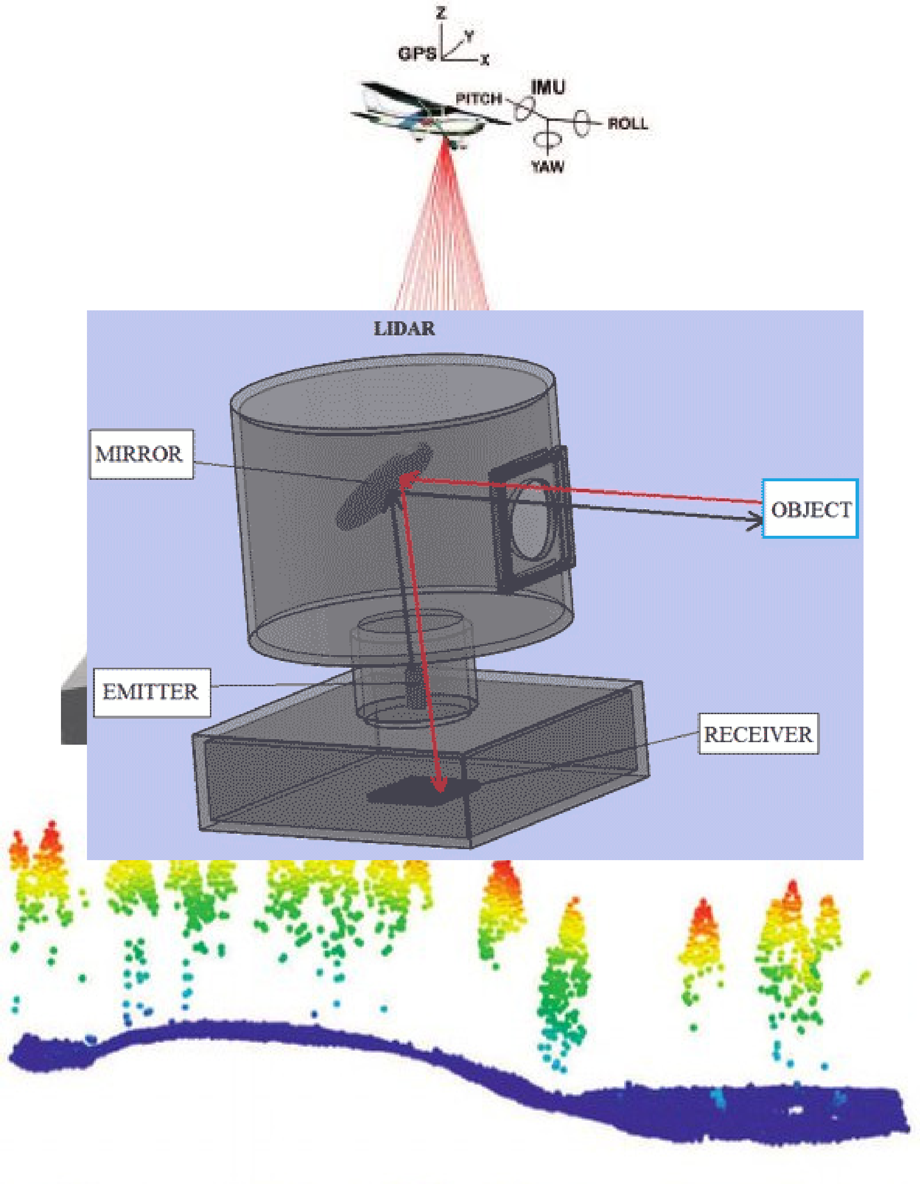

JACOBS

LiDAR returns

- Laser pulses reflect from objects both on and above the ground surface
- One pulse can be split into many returns
- First returned pulse is the most significant and will be the highest feature
- Last return may be the ground surface

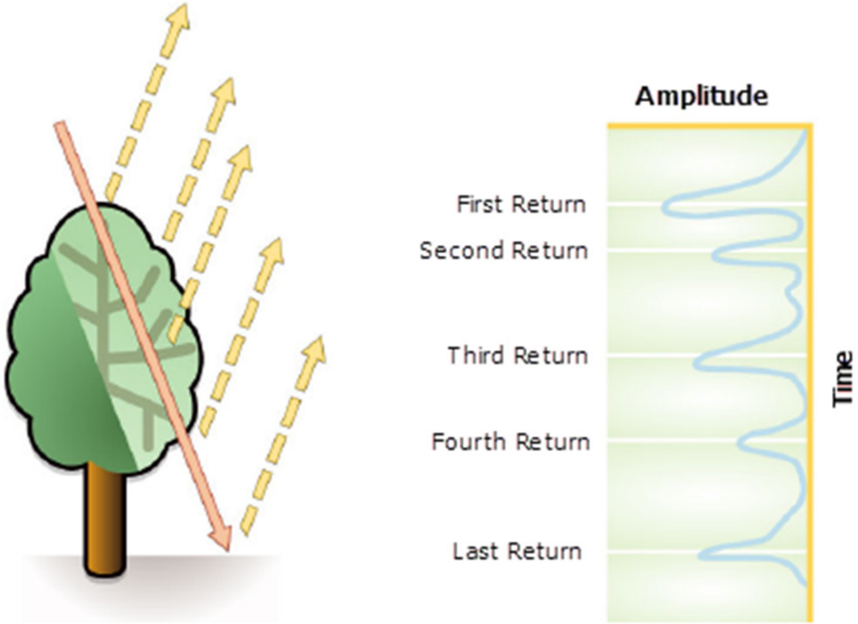

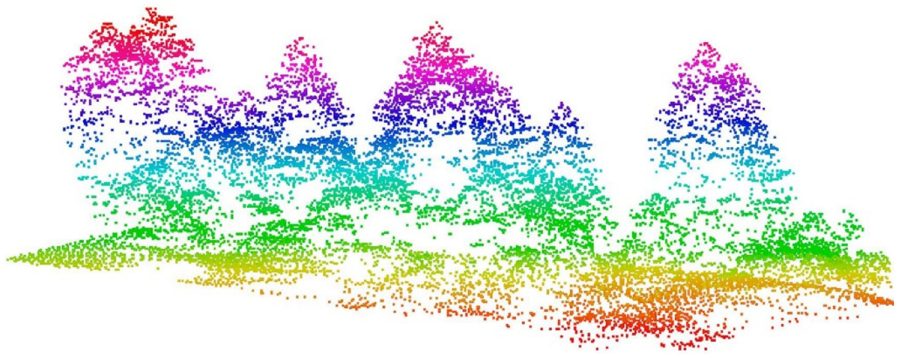

DSM vs DTM

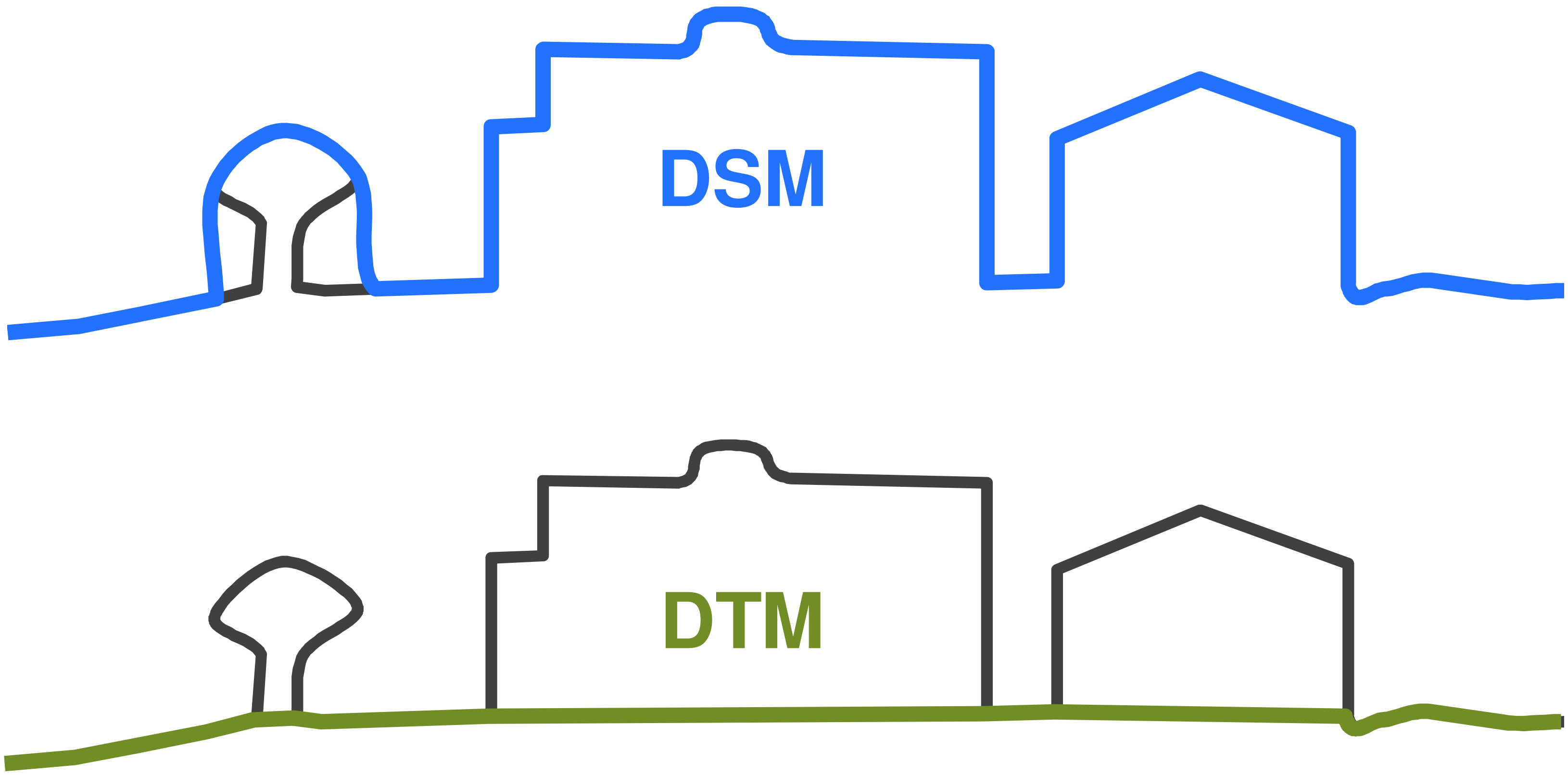

In practice…

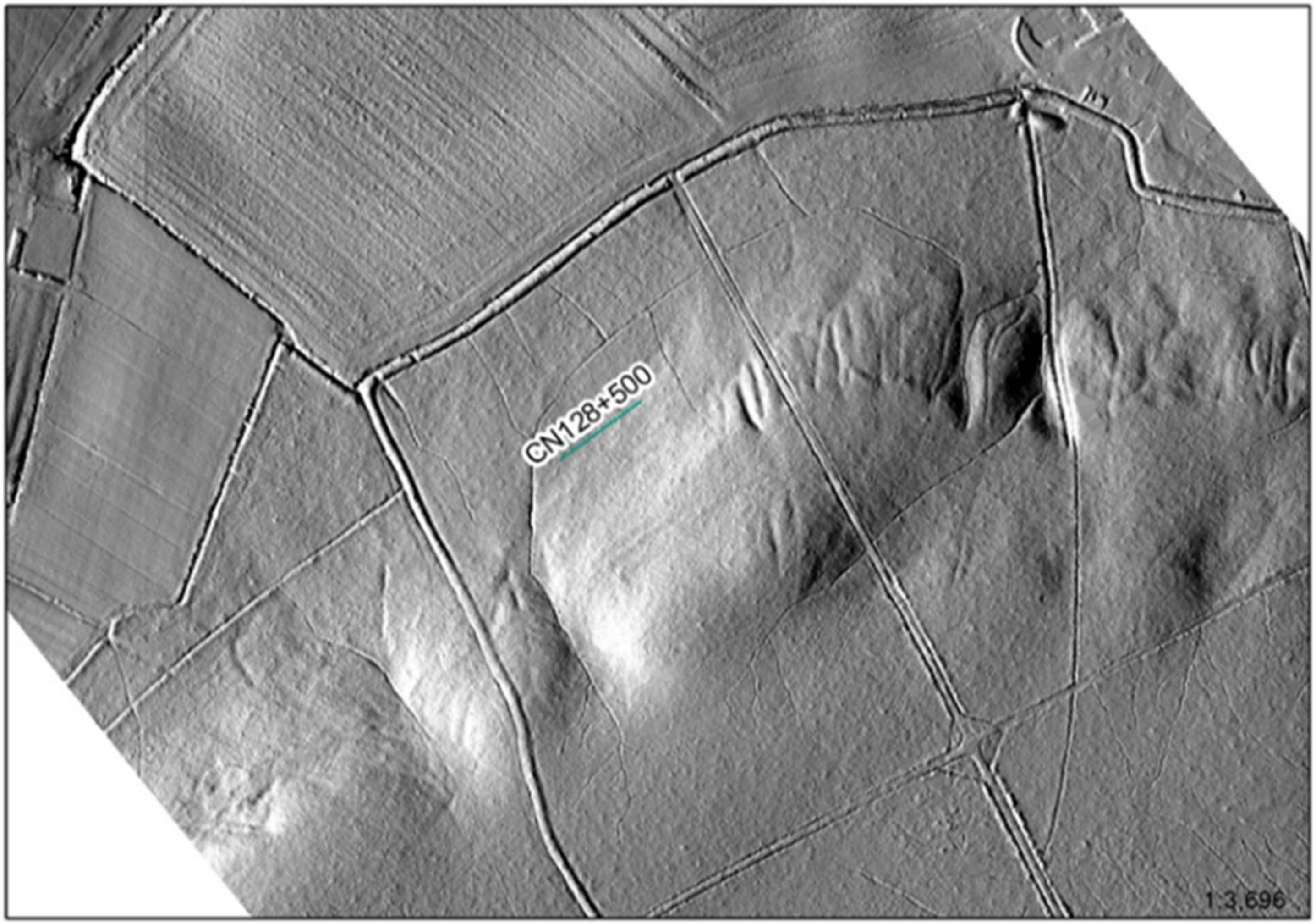

Shallow instability

- Landslide shown on BGS 50k mapping
- Evidence of a bench at/near the interface between the Penarth Group and the Mercia Mudstone
- Several surface runout channels are visible in the LiDAR imagery, suggesting that water is important
- Landslide reactivation hazard?

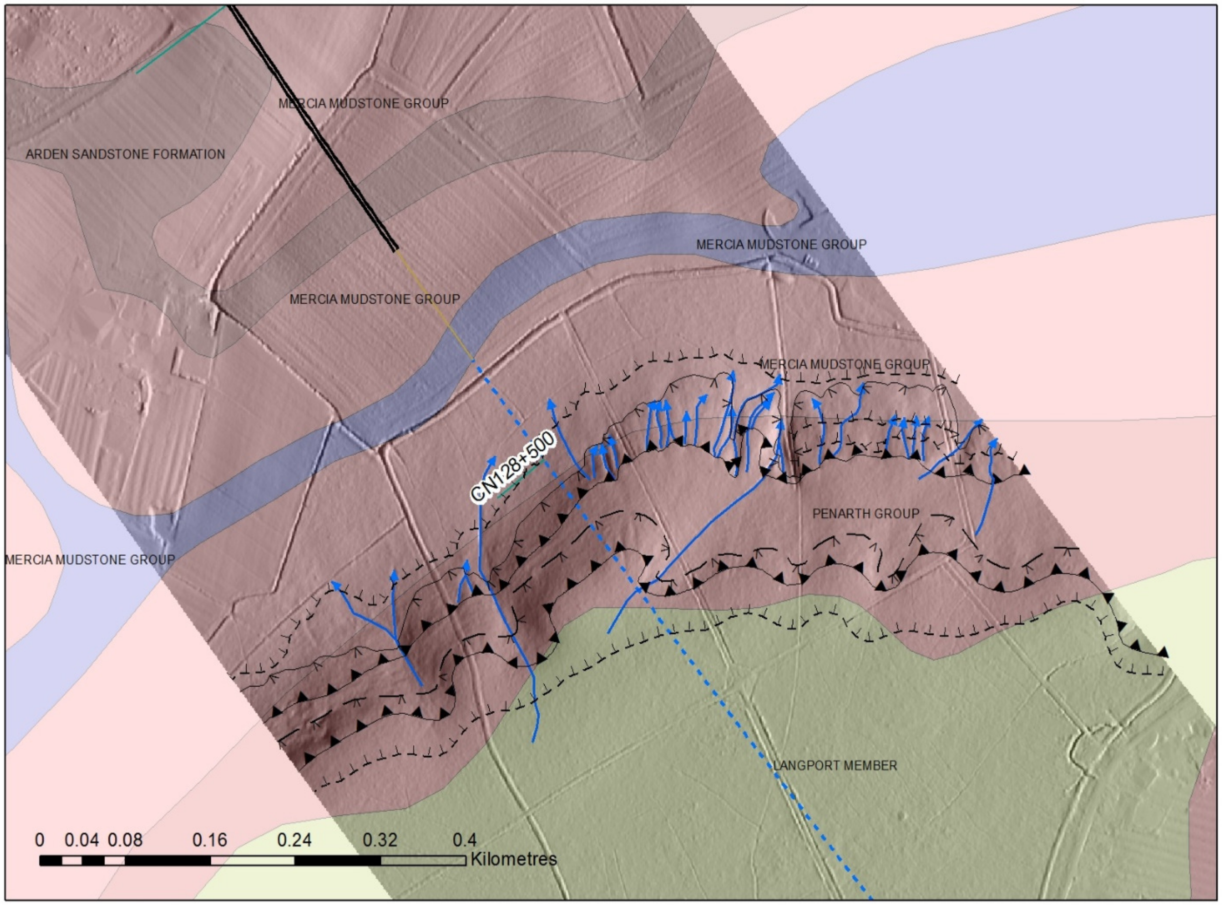

Deep instability

- Possible cambered blocks on eastern valley sidewall (A)
- Shallow mudslide embayments associated with springs (B)
- Depression in Taynton Limestone (probably a former shallow quarry) (C)

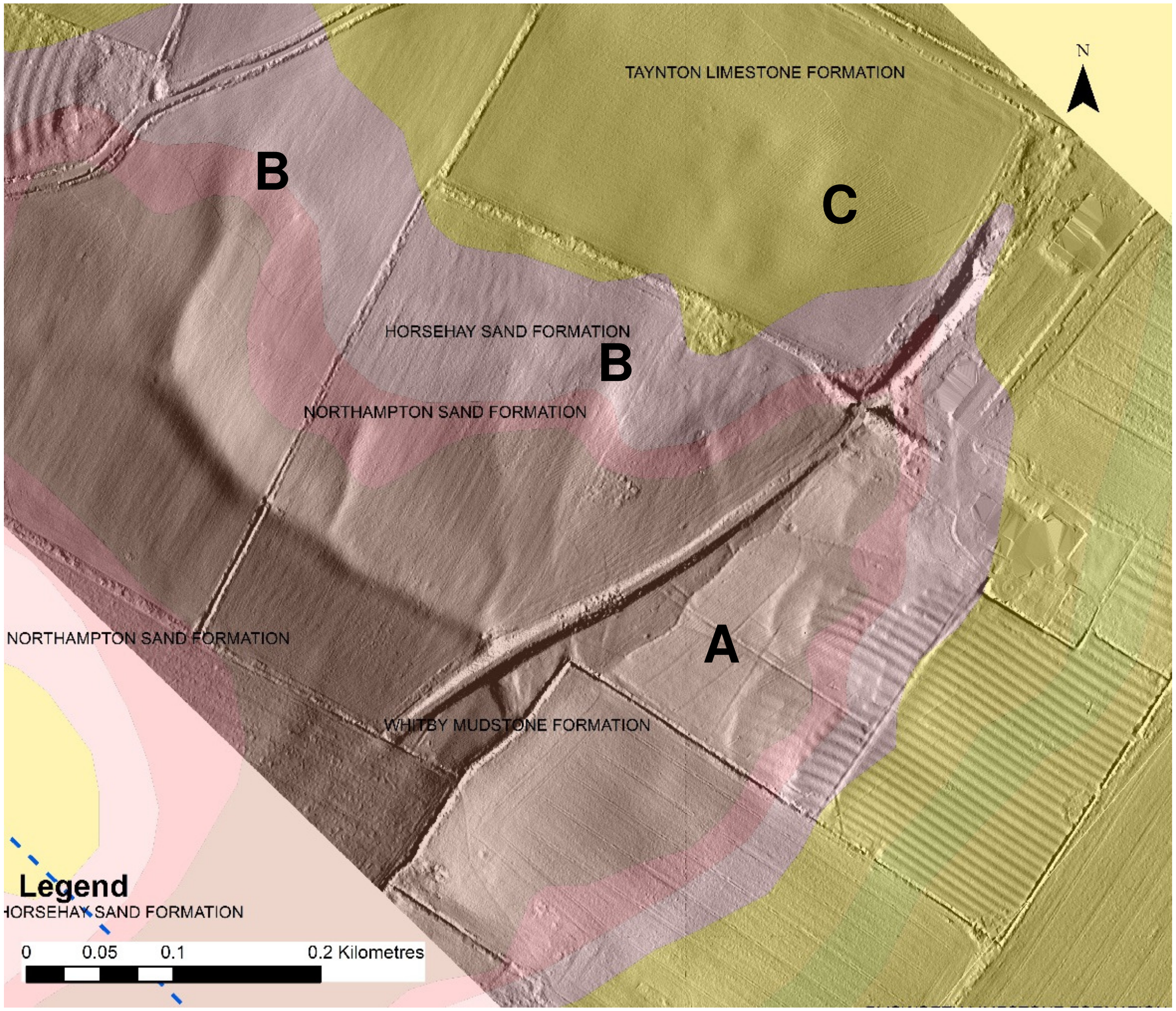

JACOBS

Example: Exeter to Newton Abbot, Network Rail

- To develop a Resilience Strategy that identifies a holistic long-term asset management pathway for the EX2NA rail line
- Geotechnical challenges included:
  - Cut-back of coastal cliffs in the 1850s
  - Minimal design, rapid construction
  - History of engineering works and past failures

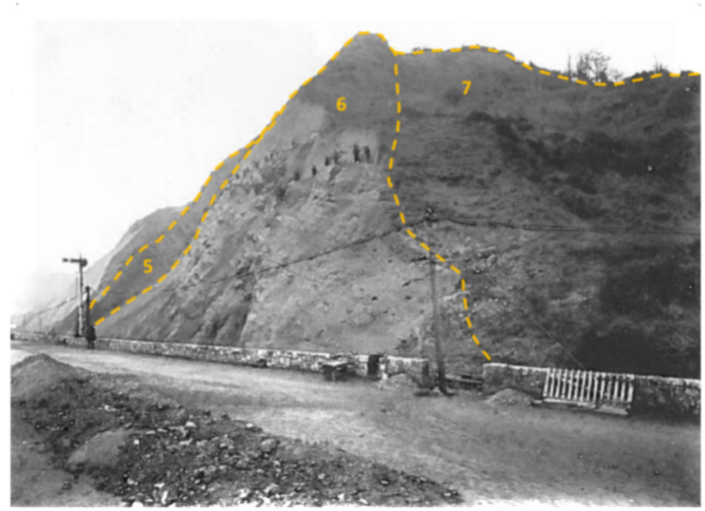

Woodlands Avenue failure, March 2014

Using LiDAR to uncover terrain

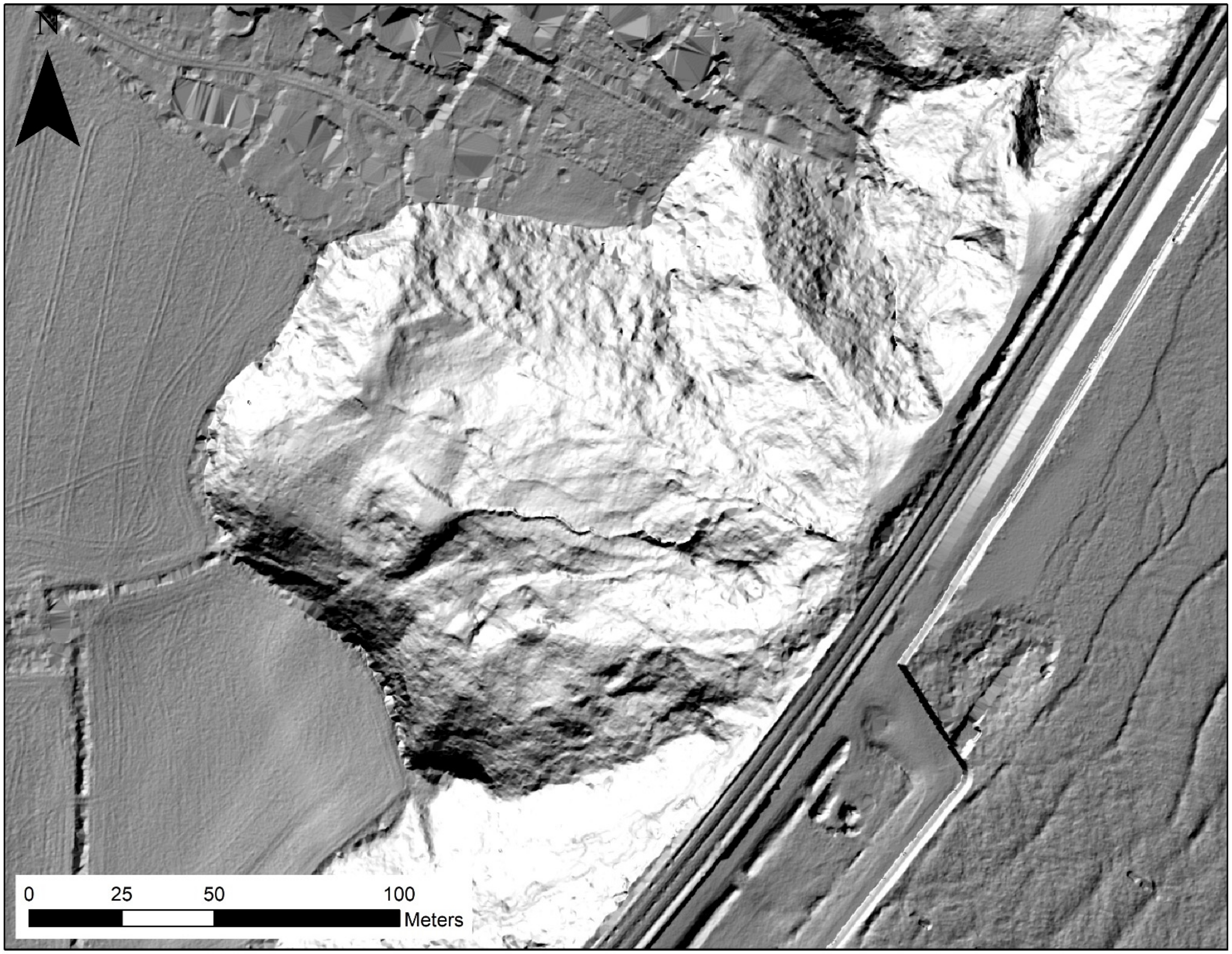

JACOBS

Terrain classification – cliff behaviour units (CBUs)

- CBUs provide an important spatial framework for defining:
  - Principal cliff failure mechanisms
  - Cliff morphology and processes
  - Geology and materials
  - External influences (surface/groundwater, toe erosion)
  - Existing stabilisation measures
  - Geotechnical asset data
- Expert panel review of conceivable cliff failure event scenarios provides indicative hazard rating for CBU

Terrain classification – cliff behaviour units (CBUs)

CBU 10 Woodland Avenue

Network Rail Chainage and National Grid Reference

Start: 207m 76.5ch (E295237 N74204)
End: 207m 72.5ch (E295286 N74274)

Hazard Rating

HIGH

(Low = negligible impact. Medium = line affected for <48 hours. High = line affected for >48 hours or potential loss of life)

Principal Hazard Mechanism
Deep-seated failure (upper cliff)

Geology (Bedrock and Superficial)
Alphington & Heavitree Breccia Formation - breccia. Upper cliff formed in deeply-weathered breccia

Photograph (March 2015)

Slope Transects

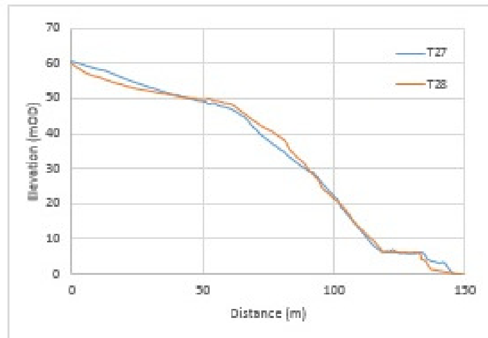

Map 1: Digital elevation model (LiDAR 2014)

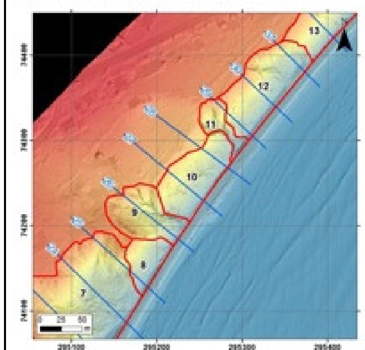

Cliff Morphology, Mechanics and Dominant Processes
The present cliff morphology is largely a result of slope regarding following the March 2014 landslide; however, two general morphological units can be observed. The upper and lower cliffs are separated by a shallow angle bench that slopes at c. 20 degrees towards the northeast (broadly coincident with the geological dip). Below this bench, the lower cliff has been regraded to a uniform c. 40 degree slope, but the cliff toe is mantled by a series of small debris lobes. The upper cliff is a marginally shallower angle uniformly regraded slope. The BGS map shows the CBU is bisected by a fault that is normal to the coastline, but this is not evident in the field. The cliff has been interpreted as a composite landslide, with a bedding-controlled translational failure in the upper part and rockslope failure / rockfall in the lower part. The associations of the two systems are unclear. A high level of antecedent rainfall is thought to have triggered the failure

Historical Events (Date and Description)
1920 rockfall
Deep-seated failure in March 2014

External Linkages (Surface Water, Groundwater and Beach)
Seepage evident from cliff, which may relate to water jetting undertaken to remove landslide debris during stabilisation. Surface water drainage is towards the cliff top in this region. The hinterland is characterised by a shallow embayment that will act to direct surface water towards the cliff top. The beach is of sand

Existing Stabilisation Measures and Hazard Mitigation Measures
Active netting across CBU
3.5m mesh catch fence with 2m wooden debris barrier across CBU

Map 2: Bedrock and Superficial Geology (Based on BGS 1:10,000 data)

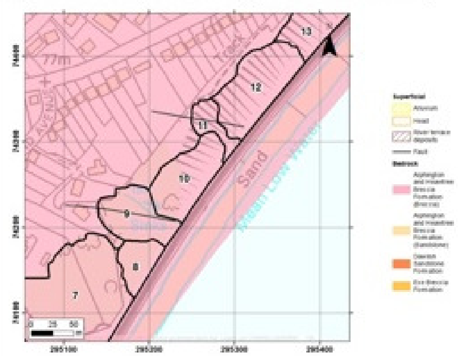

Map 3: Aerial Photo (2012)

Cliff Monitoring
6 inclinometers (non-operational; mentioned - TGP Note on Woodlands Avenue Slope Failure, 2014)
10 inclinometers;
20 piezometers (TGP Weekly Inspection Reports 2014-2015; Woodlands Phase 2 Options Report, 2015)

Cliff Inspection Records
Daily site walkovers for c. 15 weeks to note indicators of ongoing instability following stabilisation works (TGP Woodlands Phase 2 Options Report 2015)
TGP Weekly Inspection Reports (2014-2015)

Geotechnical Data
2 rotary cored boreholes (mentioned - TGP Note on Woodlands Avenue Slope Failure, 2014)
4 dynamic probes (WYGE Phase 2 Factual Report, 2003)
SPT testing; packer tests (mentioned - TGP Woodlands Phase 2 Options Report, 2015)

Historical Photo (August 1958)

JACOBS

Hazard ratings and further study

- **High hazard (line affected for >48 hours or potential loss of life)**
  - Routine inspections and maintenance, plus:
  - Cliff mapping to facilitate extensions to existing meshing and fencing
  - Intrusive ground investigations
  - Hydrological and hydrogeological study
- **Medium hazard (line affected for <48 hours)**
  - Routine inspections and maintenance, plus in some areas:
  - Further specialist inspections from track level
  - Cliff mapping and survey of some areas to facilitate extensions to existing meshing and fencing works
  - Drainage study
- **Low hazard (negligible impact)**
  - Routine inspections and maintenance
  - Limited surveys to facilitate possible extensions to fencing

Future work: Risk

- Understanding the nature of the cliff processes with LiDAR allows for a relative ranking of hazard frequency and preconditioning factors

- Data on exposure to hazard and consequence of hazard at different scales will allow for semi-quantitative risk calculation

- However, inherent limitations of LiDAR made the characterisation of geohazards in some locations very difficult

Vertical cliffs

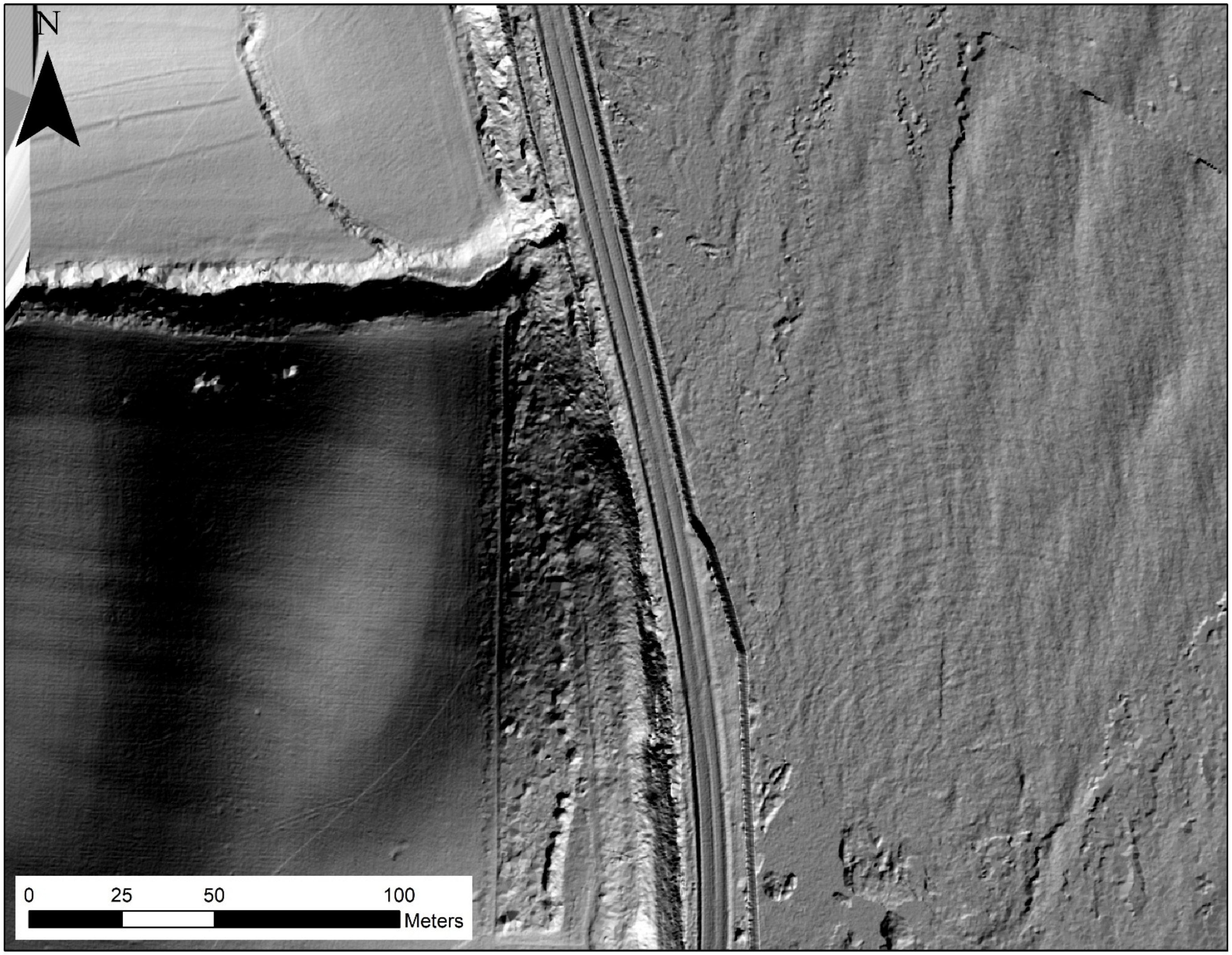

JACOBS

?

Photogrammetry – data acquisition

Photogrammetry – UAV deployment (Telscombe cliffs)

	Camera (lens)		
	Sony DSC-H300 (35X optical zoom lens)	Nikon D810 (AF-S Nikkor 24-120mm 1:4 G ED)	Nikon D810 (AF Nikkor 35mm f/2D)
			
Megapixels	20.1MP	36.3MP	36.3MP
Frame size	1/2.3" Super HAD CCD	Full frame (35.9 x 24 mm) CMOS sensor	Full frame (35.9 x 24 mm) CMOS sensor
Focal length	4.5-157.5mm (zoom)	24-120mm (zoom)	24mm (prime)* 35mm (prime)**
Image Storage	JPEG	TIFF	TIFF
Capture mode	Auto	Manual	Manual

UAV model	**DJI S1000 octocopter**
Max. take-off load	10.89kg
Max. wind	10m/s
Max. altitude	1000m
Max. flight time	15 mins (with load)
Motors and type	8 motors (model 4114-11)
Batteries	Lithium polymer
Flight modes	Manual or GPS aided navigation

JACOBS

Photogrammetry – data acquisition

Photogrammetry – UAV deployment (Telscombe cliffs)

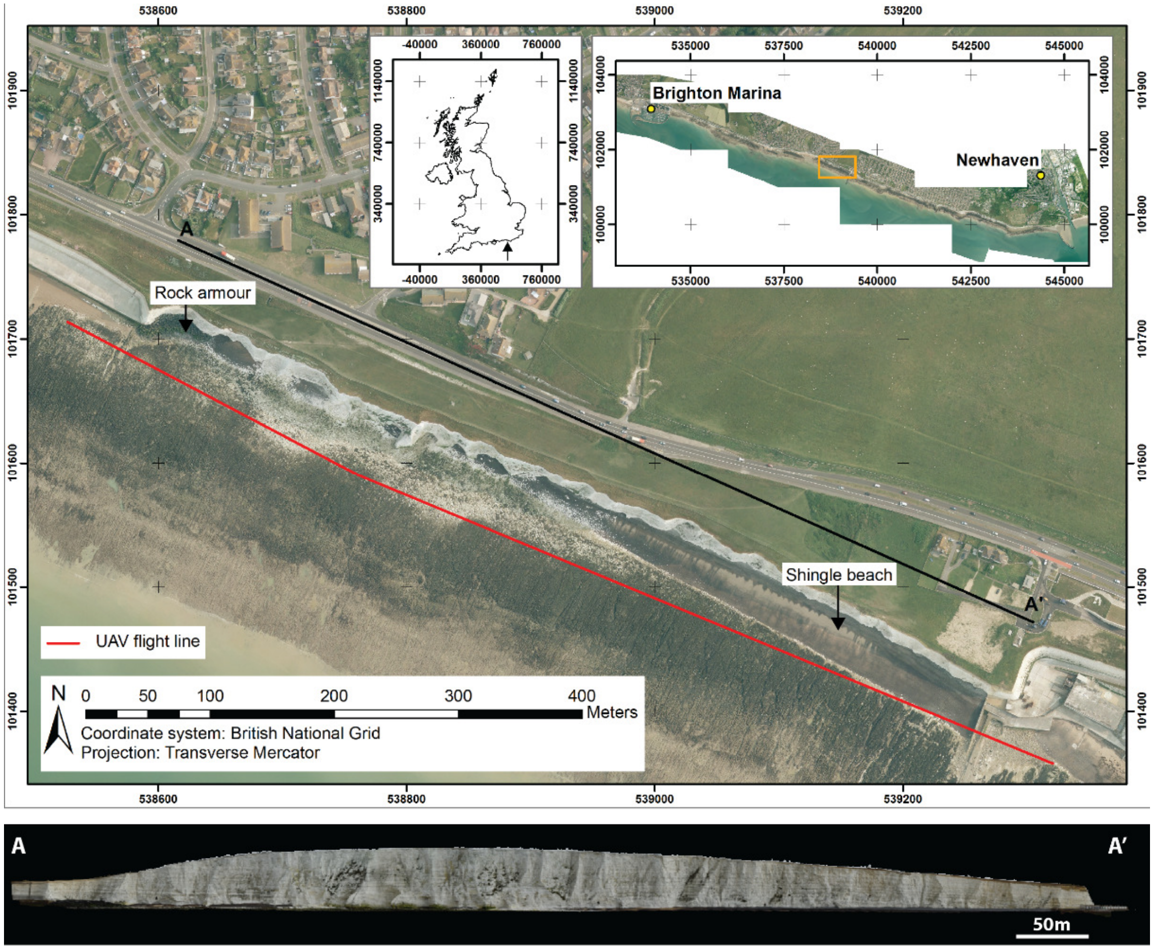

JACOBS

Photogrammetry – software

ADAM 3DM Analyst Mine Mapping Suite 2.5.0 Build 1488

Photogrammetry software platform

- 3DM Calib Cam
- DTM generator
- 3DM Analyst

Processing point clouds

- Cloud Compare

Surface change and volumetric estimations

- ArcGIS

Photogrammetry – method

Interior orientations (3DM Calib Cam)

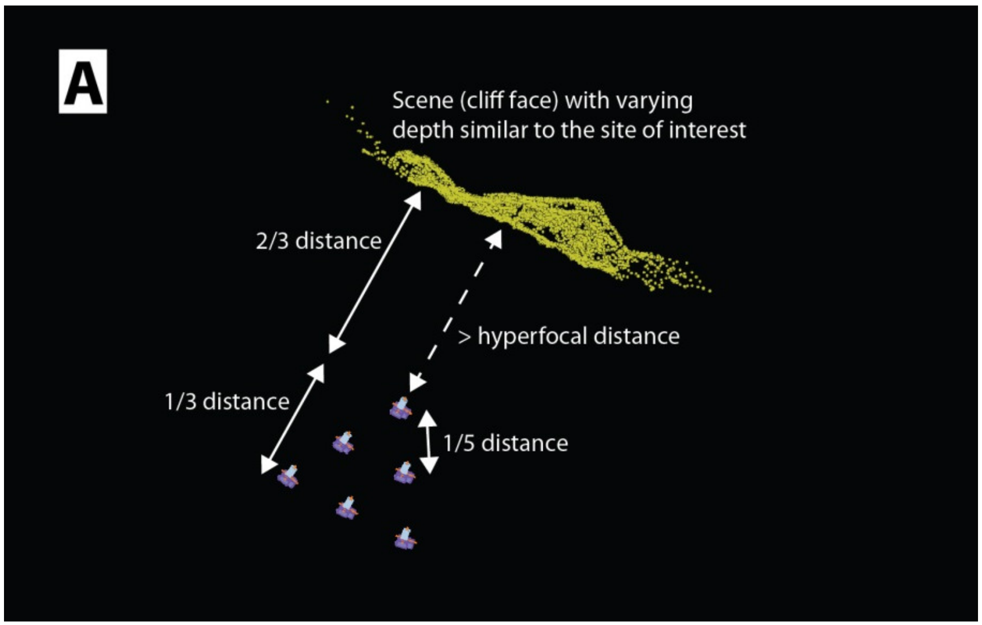

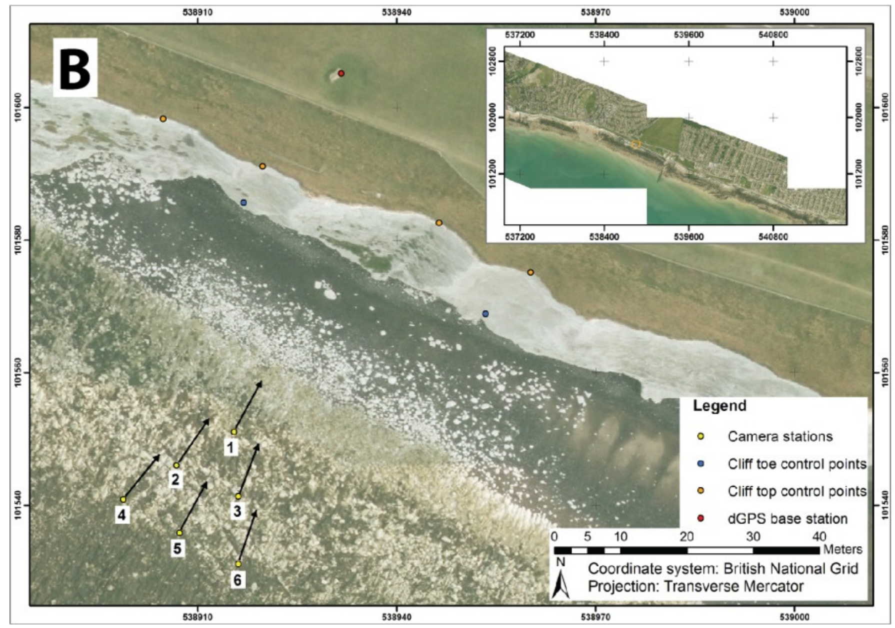

Photogrammetry – method

Interior orientations (3DM Calib Cam)

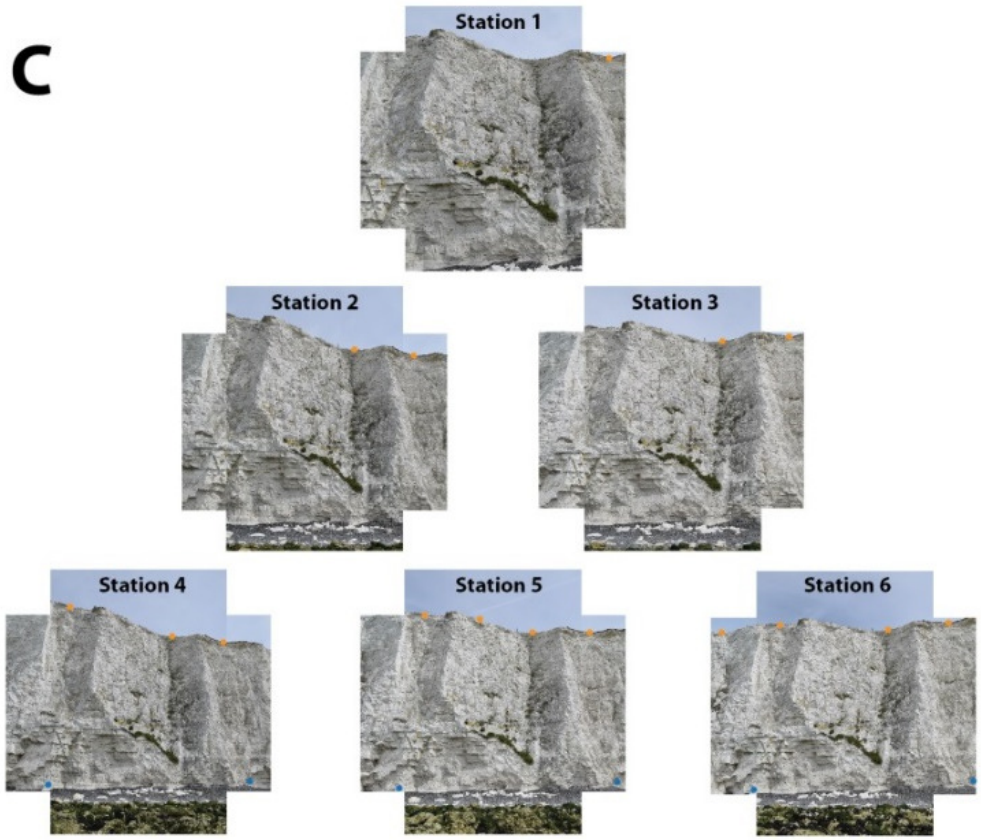

Photogrammetry – method

Exterior orientations (3DM Calib Cam)

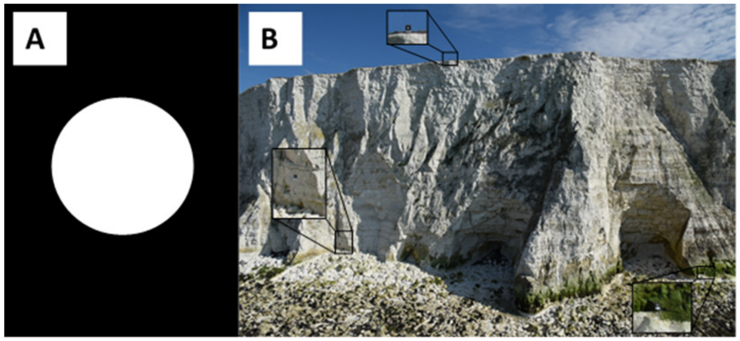

Photogrammetry – method

Exterior orientations (3DM Calib Cam)

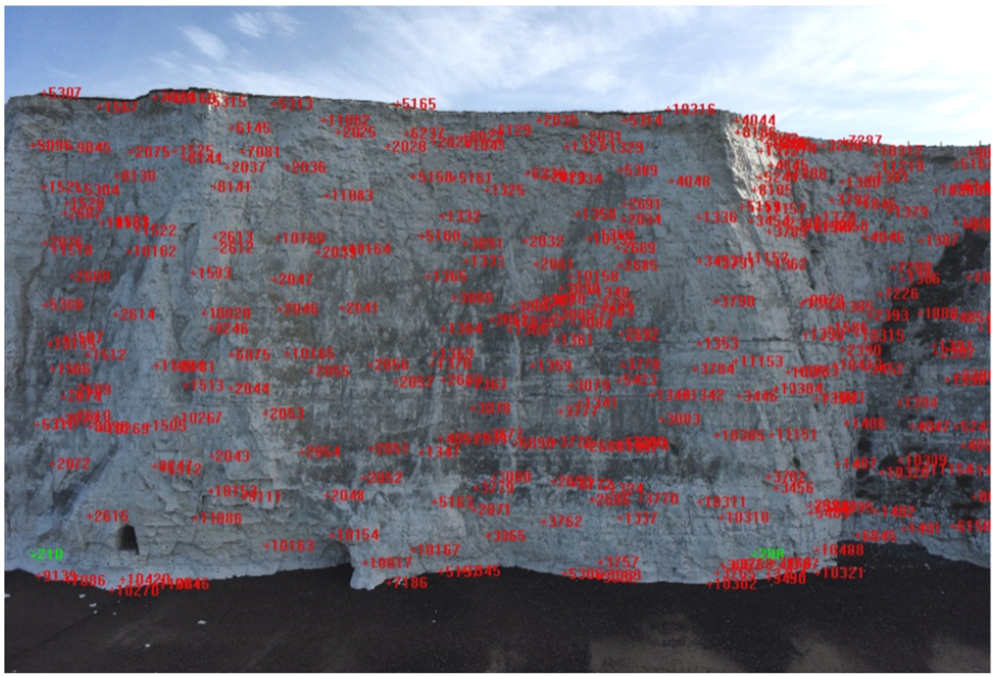

Photogrammetry – processing

Model production (DTM generator)

- DTM statistics (averaged from 12 months of data)
  - 125 DTMs
  - 32.5 million points
  - 688 pts/m^2
- Merged DTM files – point spacing 0.05m (processing capability)

JACOBS

Photogrammetry – processing

Model example (3DM Analyst)

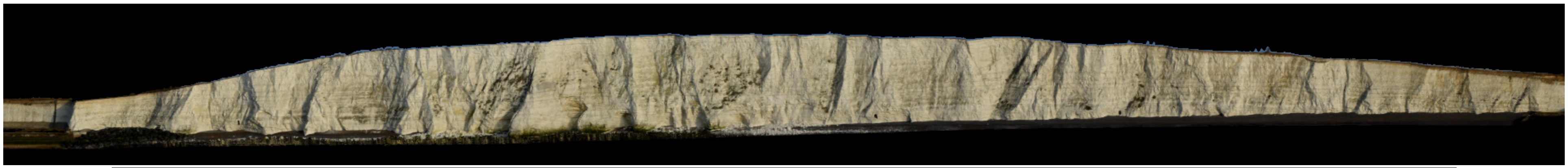

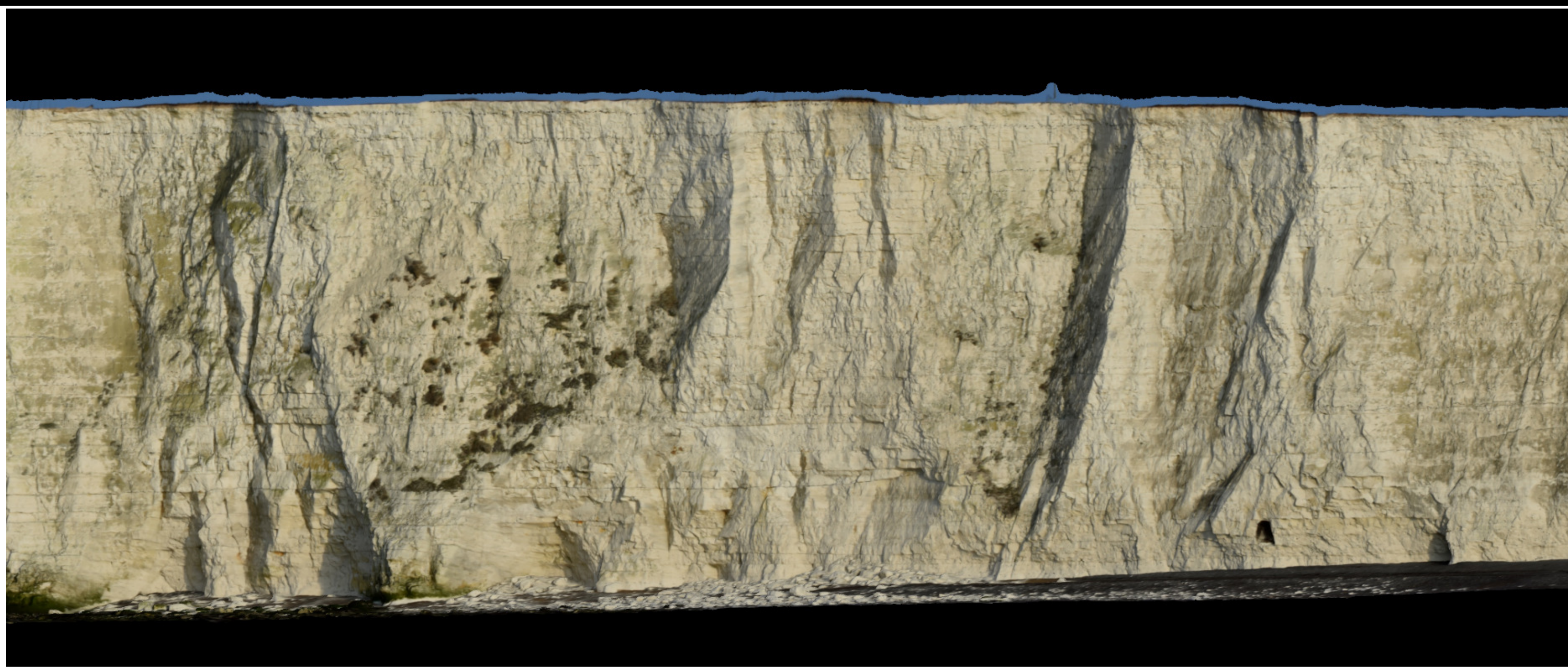

Photogrammetry – processing

- Models exported as point files
- Point clouds were transformed in CloudCompare
- Data was rasterised with a cell size of 0.1m
- 2.5D surface change detection was completed in ArcGIS
- Removal of edge effects and vegetation (false change)
- Volumetric estimations undertaken in ArcGIS

Photogrammetry – surface change

Surface change – Telscombe cliffs

Total volumetric flux 3,889.35m^3

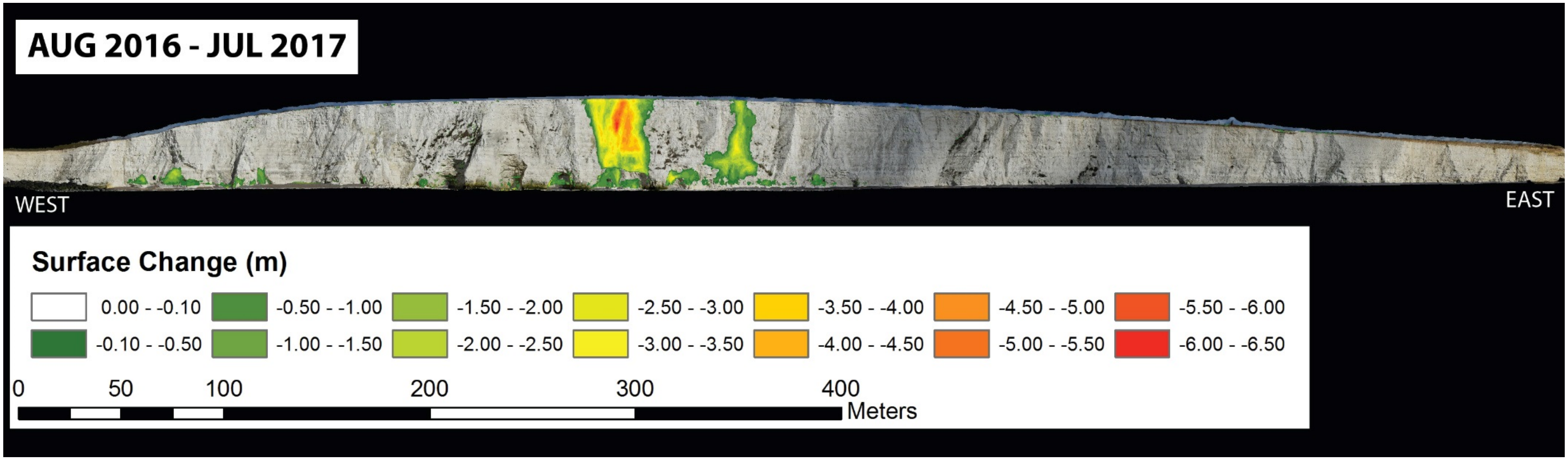

Photogrammetry – surface change

Surface change – Telscombe cliffs – successive failures
(August – December 2016)

Volumetric estimation

Aug-Sep

152.66m^3 (wedge)

47.18m^3 (arch)

Oct-Nov

37.66m^3 (block)

Nov-Dec

512.33m^3 (pillar)

38.49m^3 (arch)

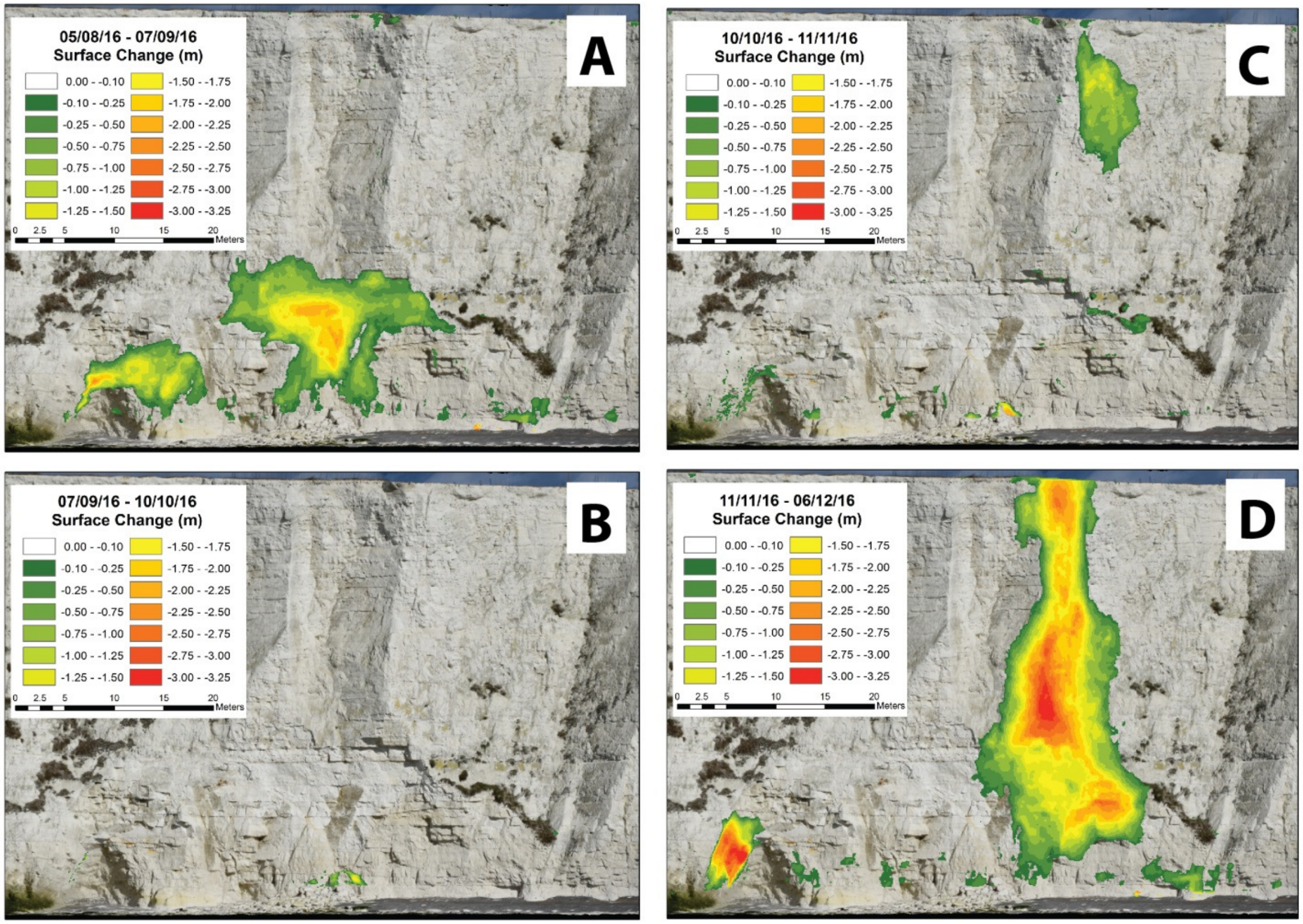

JACOBS

Photogrammetry – surface change

Surface change – Telscombe cliffs – successive failures
(August – December 2016)

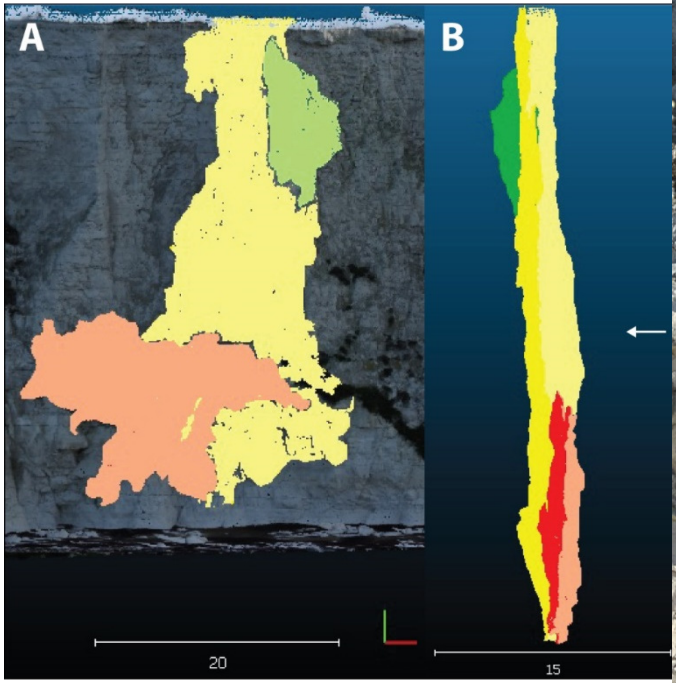

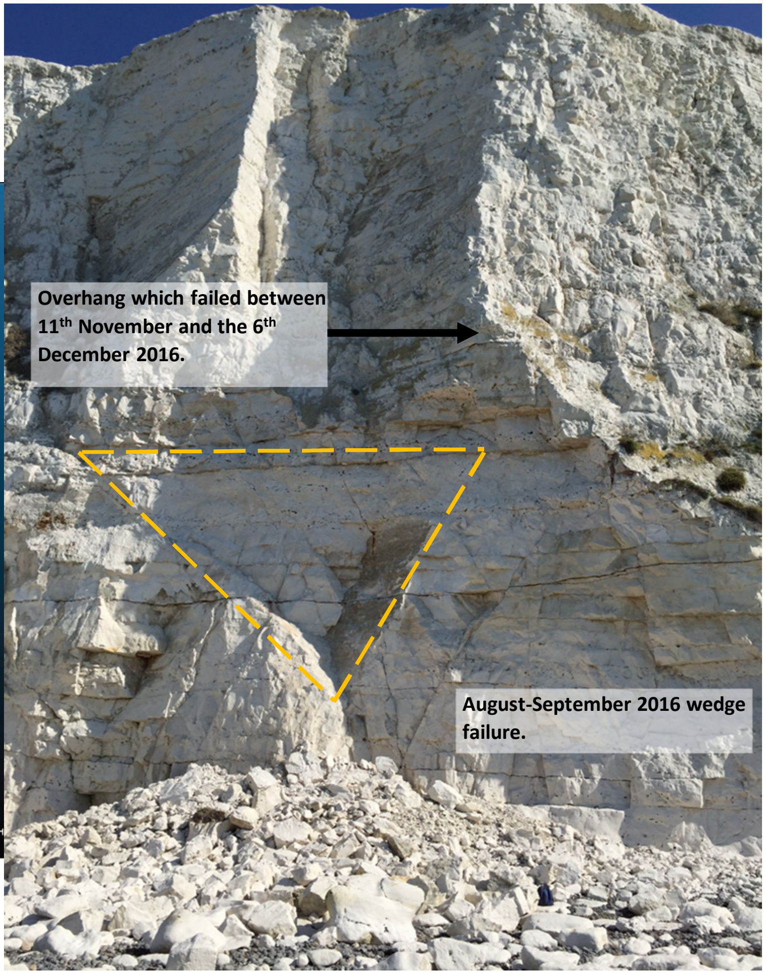

JACOBS

Photogrammetry – surface change

Surface change – Telscombe cliffs – toe erosion (August 2016 – March 2017)

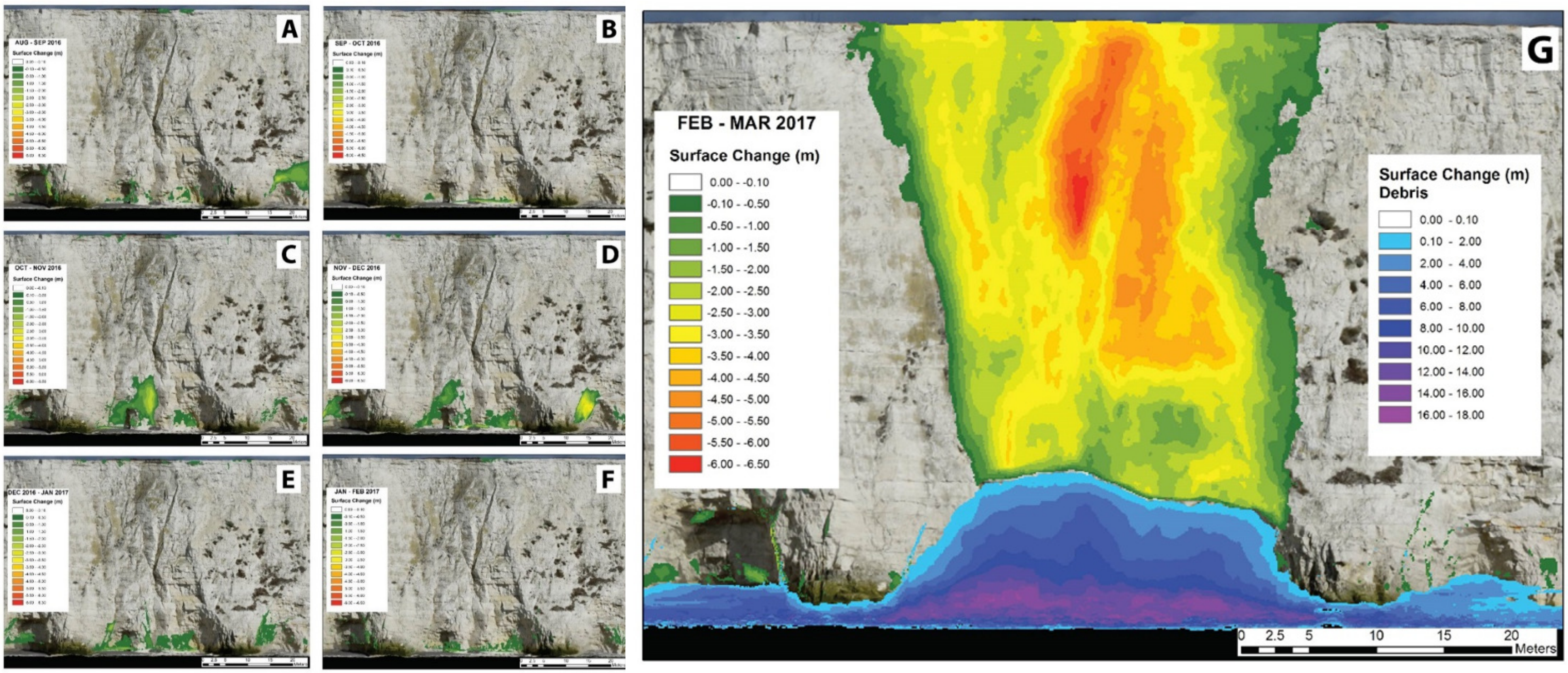

JACOBS

Photogrammetry – numerical/statistical modelling

- Probabilistic recession modelling using negative power law scaling of rockfalls and environmental controls
- Rockfall inventory captured over 12 months with a total of 10,085 mass wasting events
- Studies had previously demonstrated that negative power laws best describe landslide magnitude-frequency distributions as expressed by Brunetti et al. (2009):

$$f(V_R)=sV_R^{-\beta}$$

JACOBS

Photogrammetry – numerical/statistical modelling

- Data was logarithmically binned and normalised by space and time (km^{-2} $month^{-1}$)

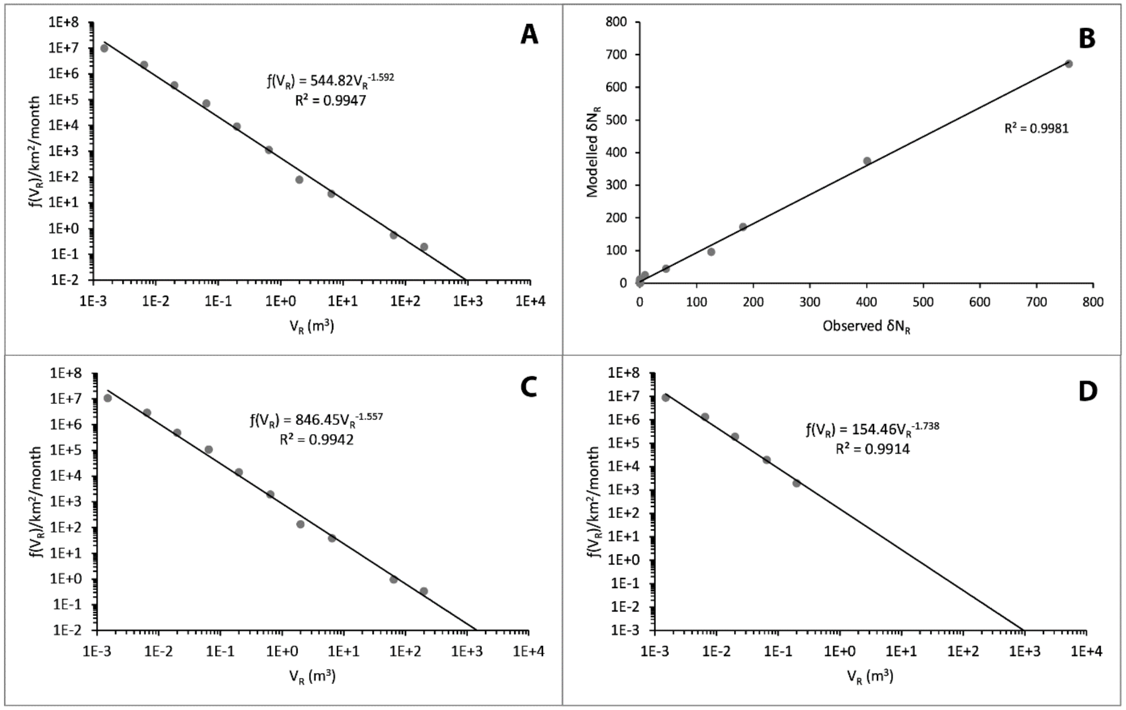

Power law estimation parameters for August to September 2016
(A) frequency density and magnitude of failures for the entire study area
(B) the predicted vs. observed frequency of failures for all binned data
(C) frequency density and magnitude of failures for the undefended section
(D) frequency density and magnitude of failures for the natural defended section (beach)

Photogrammetry – numerical/statistical modelling

$$V_T = \frac{sV_{R\,max}^{\;2-\beta}}{2-\beta} - \frac{sV_{R\,min}^{\;2-\beta}}{2-\beta}$$

- Maximum failure volume:

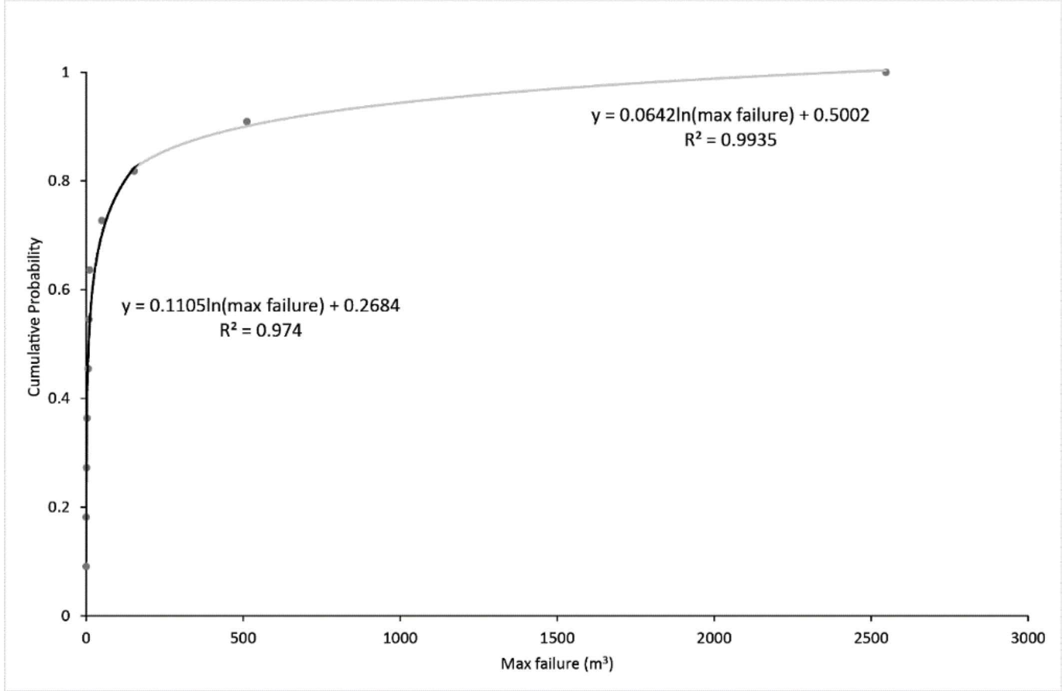

- Minimum set to 1 x $10^{-6}m^3$

JACOBS

Photogrammetry – numerical/statistical modelling

- Numerical constants of the equation were constrained by H_s

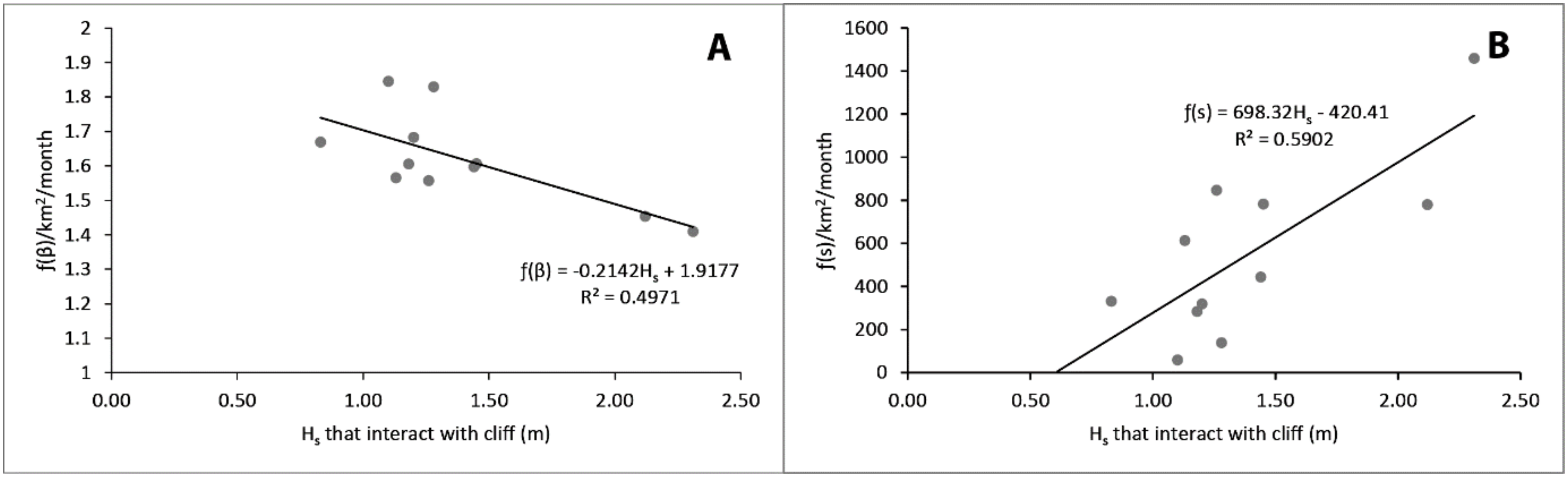

Photogrammetry – numerical/statistical modelling

Monthly and decadal probability functions of H_s were used from the UKCP09 Medium Emission Scenario (Lowe et al., 2009; Leake et al., 2009; Brown et al., 2012)

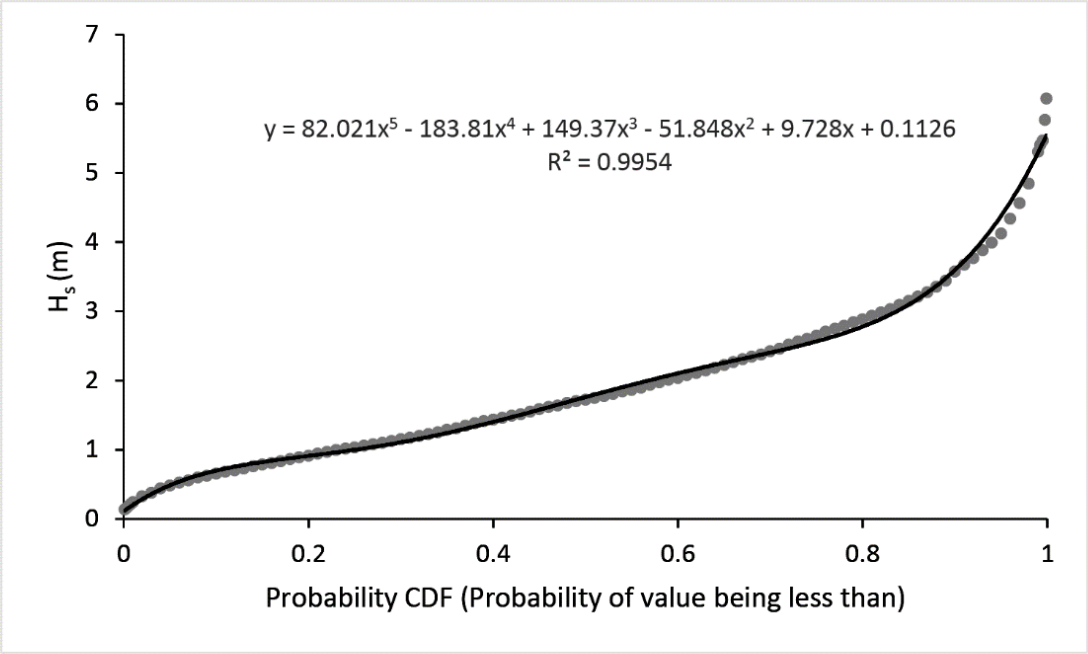

JACOBS

Photogrammetry – numerical/statistical modelling

Sea Level Rise was accounted for by a time of exposure approach

- Tidal interaction with base of cliff
- Increased from 28.58% to 33.85% for current sea level and sea level predicted in 2089
- Scaling factor applied – current condition 1 by 2089 1.0527

Photogrammetry – numerical/statistical modelling

Model run for the unprotected cliff line as the shingle beach provides substantial protection to the toe

- Unprotected site accounted for 59% of the area but 99.57% of the observed erosion

Model vs Observations

- r^2=0.9918 and the model predicted 97% of the observed V_T for this section

Monte Carlo simulation developed and run 10,000 times to determine the most likely erosion scenario

Photogrammetry – numerical/statistical modelling

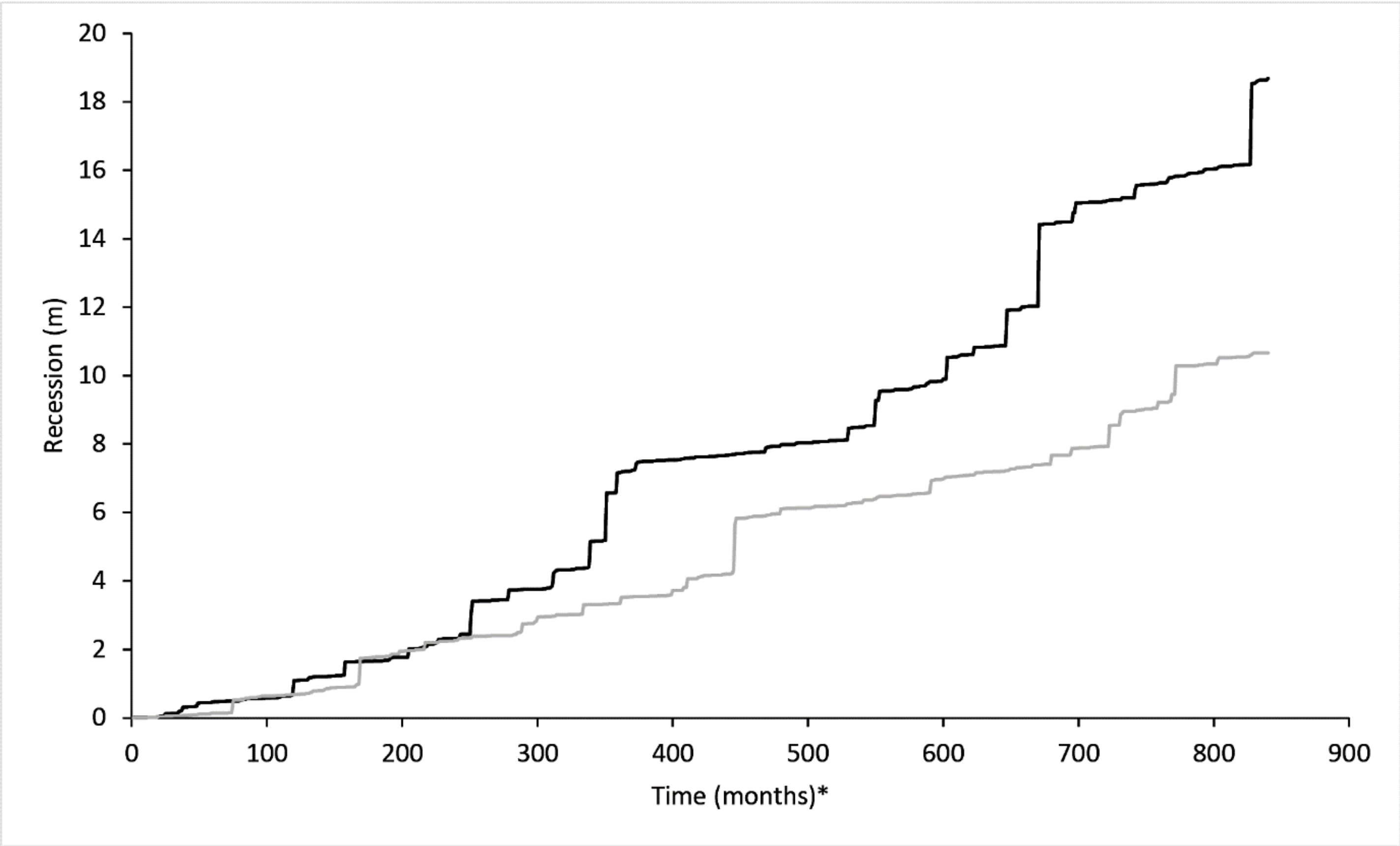

Photogrammetry – numerical/statistical modelling

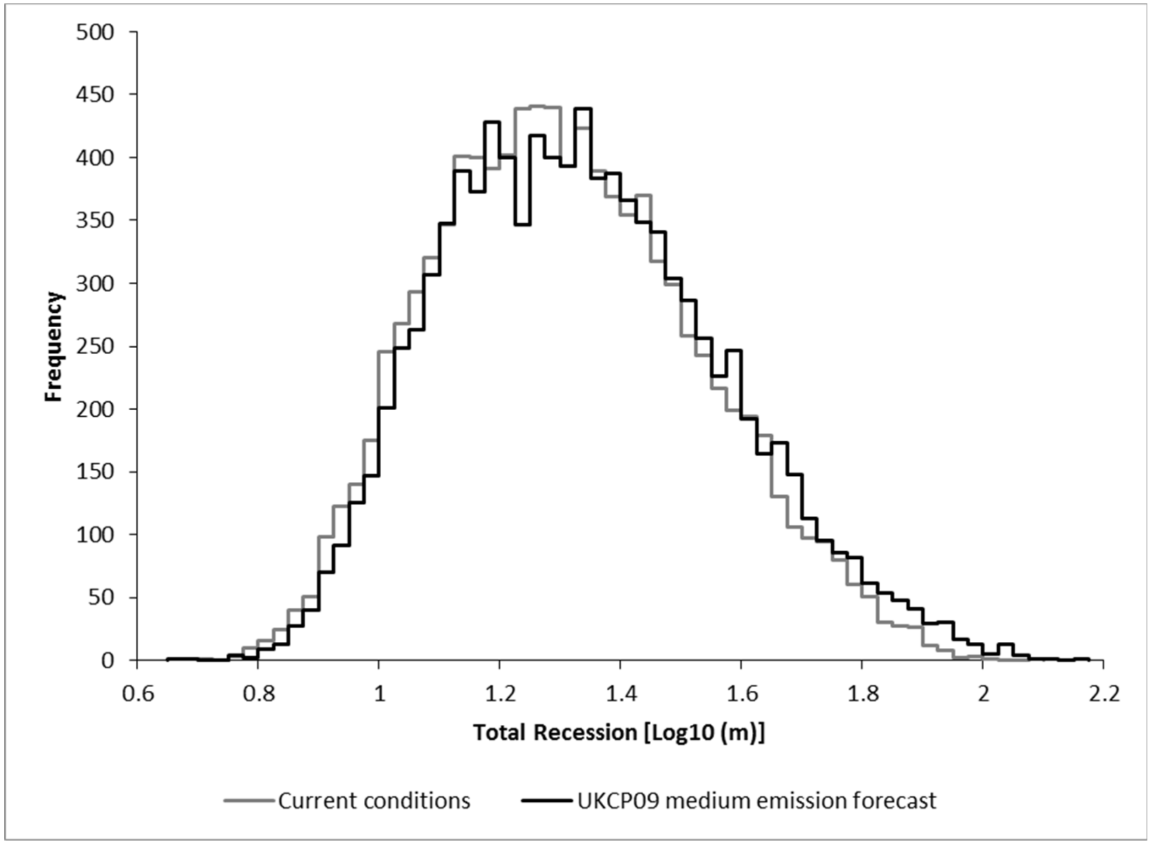

	Current Conditions		UKCP09 medium emission forecast	
	Log10	Recession (m)	Log10	Recession (m)
Average	1.311	20.45	1.338	21.76
Max	2.086	121.97	2.157	143.56
Min	0.714	5.18	0.659	4.56
95.5%CI	1.750	56.26	1.797	62.61

Photogrammetry – numerical/statistical modelling

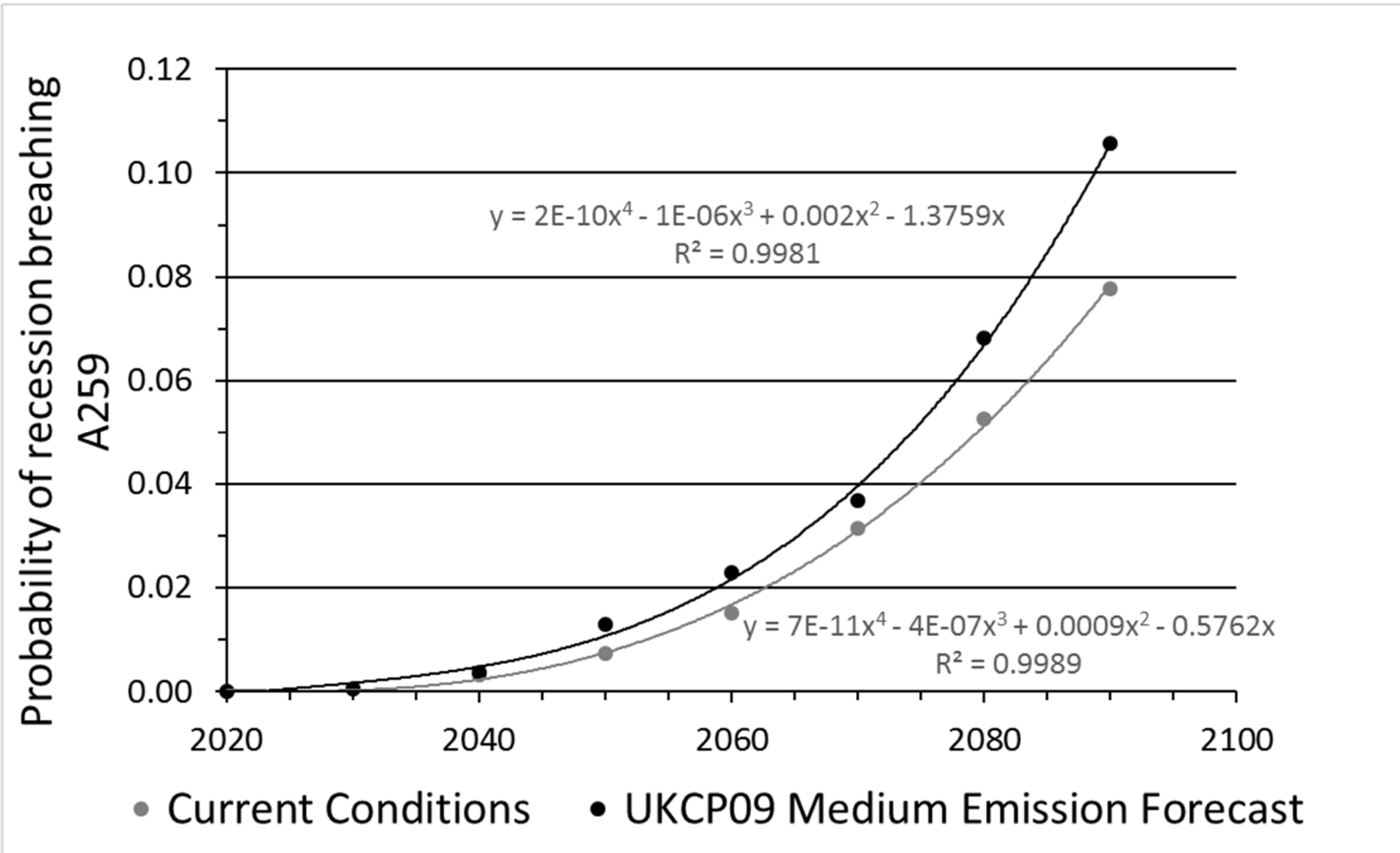

Photogrammetry – discontinuity analysis

Discontinuity mapping (3DM Analyst)

391 digitised planes

- 255 joints
  (JS1 – yellow)
  (JS2 – orange)
  (J – blue)
- 28 faults (red)
- 108 bedding planes
  (not in image)

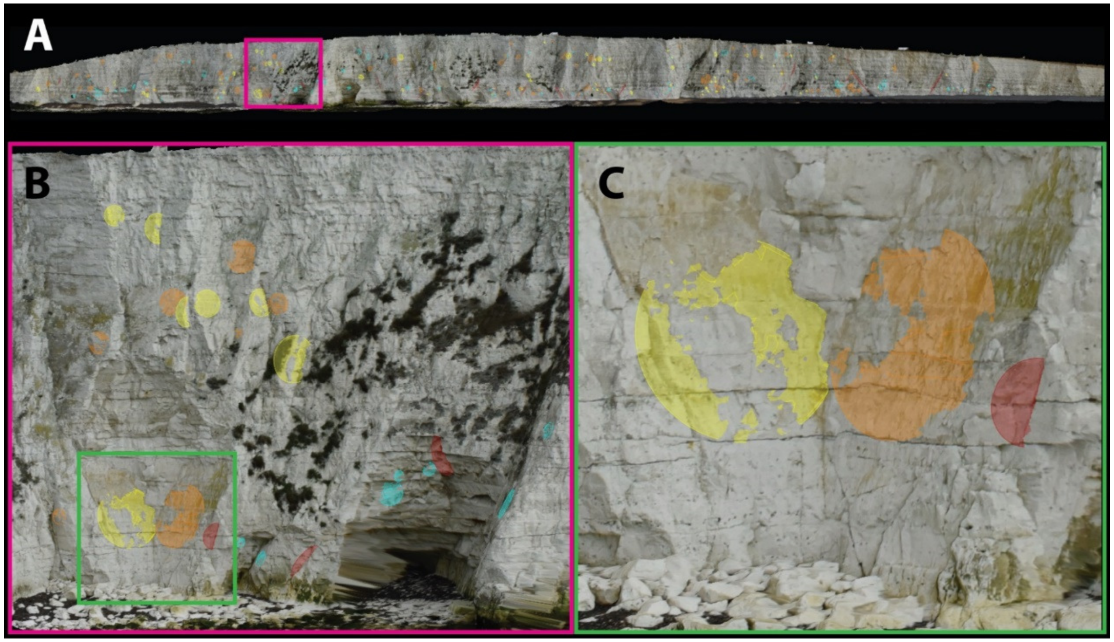

JACOBS

Photogrammetry – discontinuity analysis

Kinematic analysis (DIPS 7.0)

A

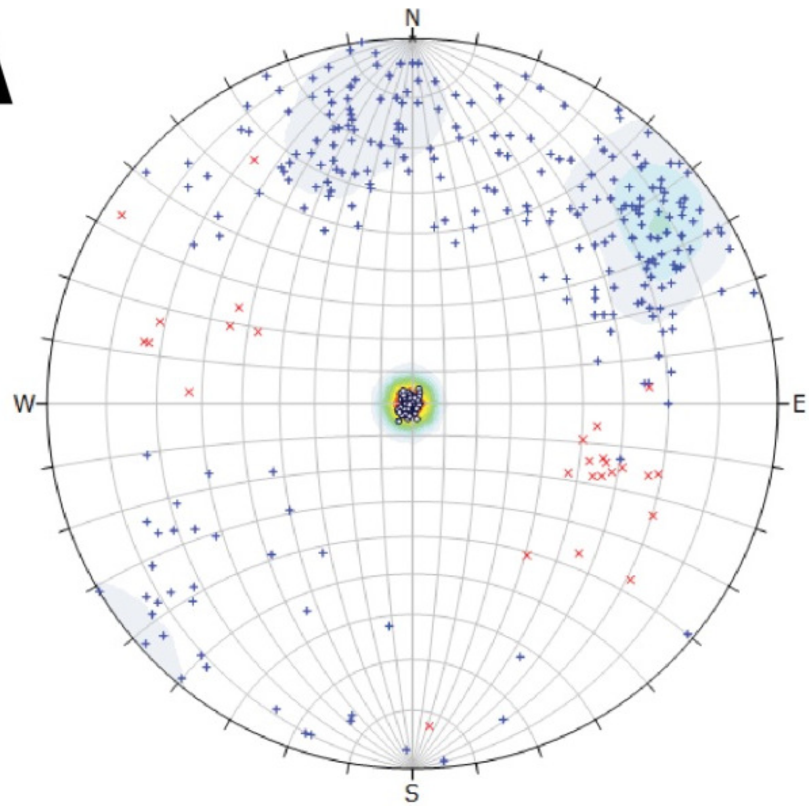

Symbol	TYPE	Quantity
o	Bedding Planes	108
×	Faults	27
+	Joints	256

Color	Density Concentrations
	0.00 - 2.70
	2.70 - 5.40
	5.40 - 8.10
	8.10 - 10.80
	10.80 - 13.50
	13.50 - 16.20
	16.20 - 18.90
	18.90 - 21.60
	21.60 - 24.30
	24.30 - 27.00

Contour Data	Pole Vectors
Maximum Density	26.73%
Contour Distribution	Fisher
Counting Circle Size	1.0%
Plot Mode	Pole Vectors
Vector Count	391 (391 Entries)
Hemisphere	Lower
Projection	Equal Angle

Photogrammetry – discontinuity analysis

Kinematic analysis (DIPS 7.0)

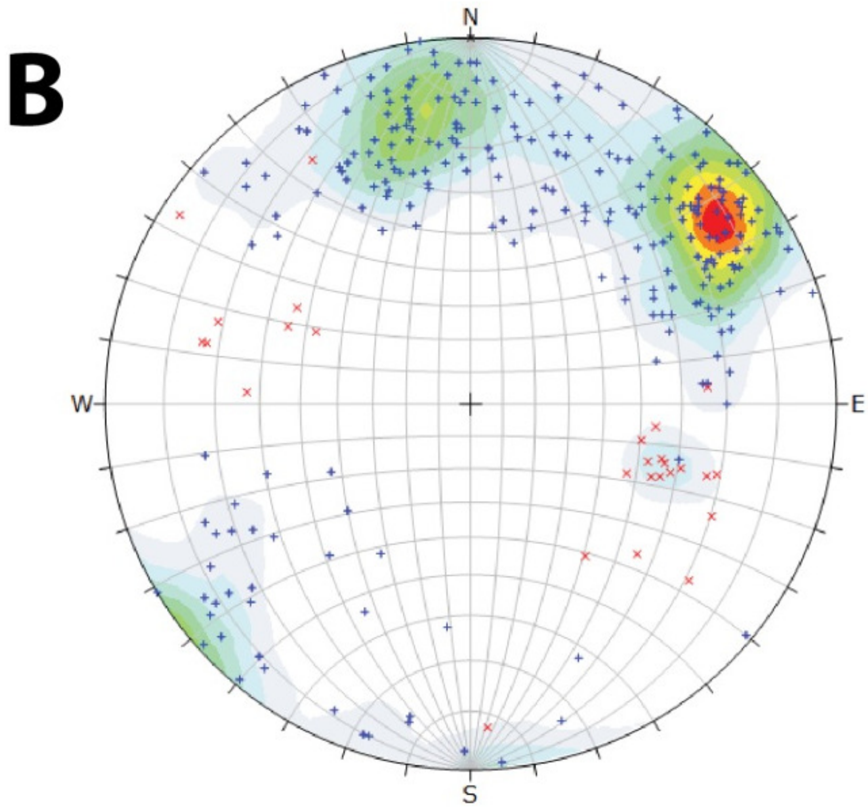

Symbol	TYPE	Quantity
×	Faults	27
+	Joints	256

Color	Density Concentrations
	0.00 - 1.20
	1.20 - 2.40
	2.40 - 3.60
	3.60 - 4.80
	4.80 - 6.00
	6.00 - 7.20
	7.20 - 8.40
	8.40 - 9.60
	9.60 - 10.80
	10.80 - 12.00

Contour Data	Pole Vectors
Maximum Density	11.86%
Contour Distribution	Fisher
Counting Circle Size	1.0%

Plot Mode	Pole Vectors
Vector Count	283 (283 Entries)
Hemisphere	Lower
Projection	Equal Angle

Photogrammetry – discontinuity analysis

Kinematic analysis (DIPS 7.0)

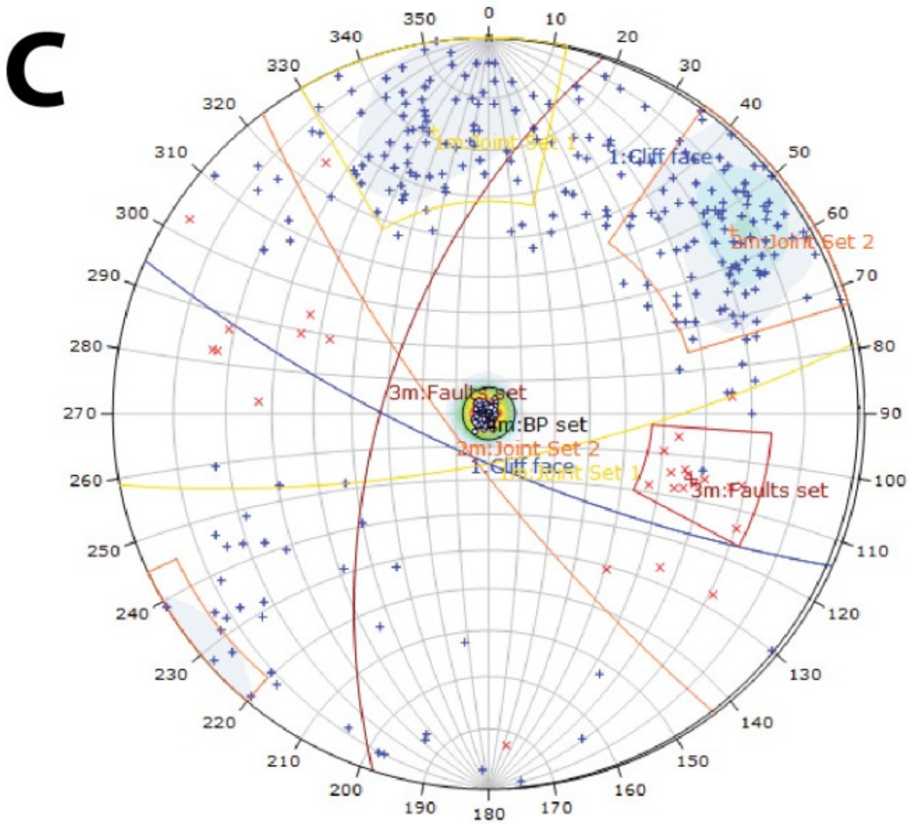

Symbol	TYPE	Quantity
∘	Bedding Planes	108
×	Faults	27
+	Joints	256

Color	Density Concentrations
	0.00 - 2.70
	2.70 - 5.40
	5.40 - 8.10
	8.10 - 10.80
	10.80 - 13.50
	13.50 - 16.20
	16.20 - 18.90
	18.90 - 21.60
	21.60 - 24.30
	24.30 - 27.00
Contour Data	Pole Vectors
Maximum Density	26.73%
Contour Distribution	Fisher
Counting Circle Size	1.0%

	Color	Dip	Dip Direction	Label
User Planes				
1		76	204	Cliff face
Mean Set Planes				
1m		75	169	Joint Set 1
2m		78	233	Joint Set 2
3m		59	288	Faults set
4m		1	87	BP set

Photogrammetry – discontinuity analysis

Percentage of mapped intersections favourable to mode:

- Wedge - 39.97%
  - 27.82% (primary)
  - 12.15% (secondary)
- Planar – 7.16%
- Flexural – 0.31%

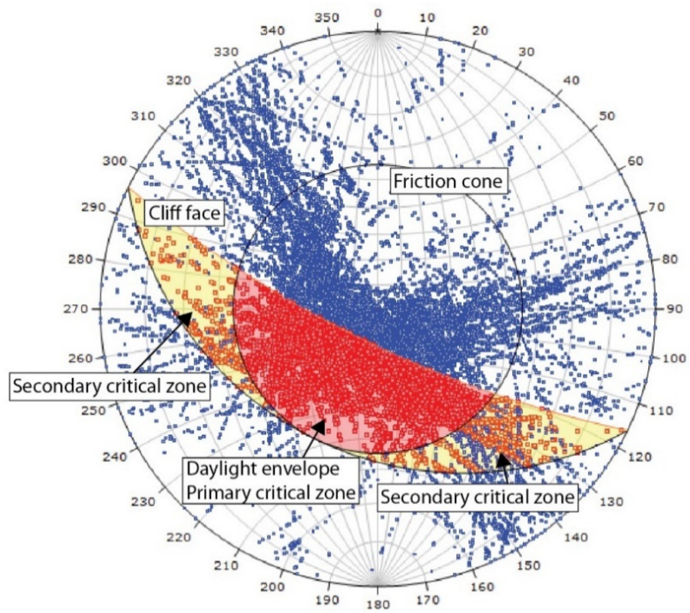

Symbol	Feature
•	Critical Intersection
•	Intersection

Kinematic Analysis	Wedge Sliding
Slope Dip	76
Slope Dip Direction	206
Friction Angle	35°

	Critical	Total	%
Wedge Sliding	15946	39899	39.97%

Plot Mode	Pole Vectors
Vector Count	283 (283 Entries)
Intersection Mode	Grid Data Planes
Intersections Count	39899
Hemisphere	Lower
Projection	Equal Angle

Photogrammetry – discontinuity analysis

Wedge failure – analysis

Estimated volume – 2546.84m^3

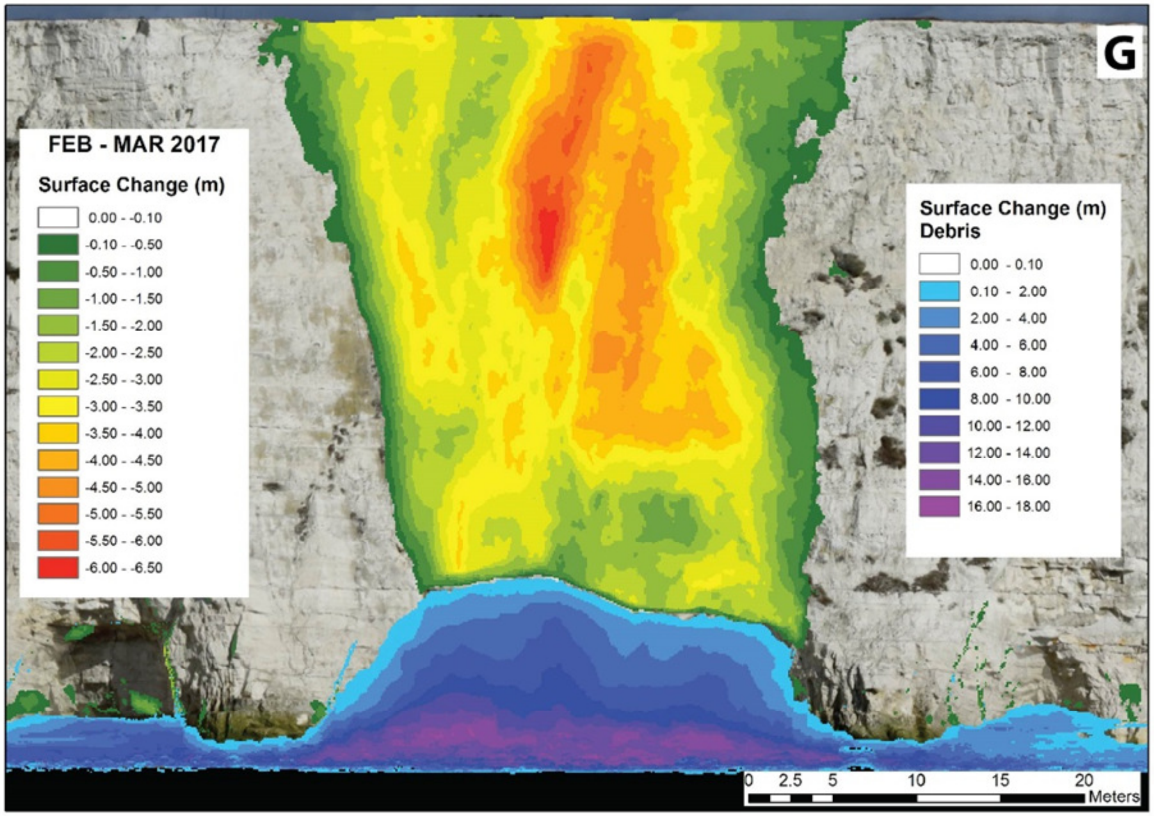

Photogrammetry – discontinuity analysis

Wedge failure – analysis (Swedge)

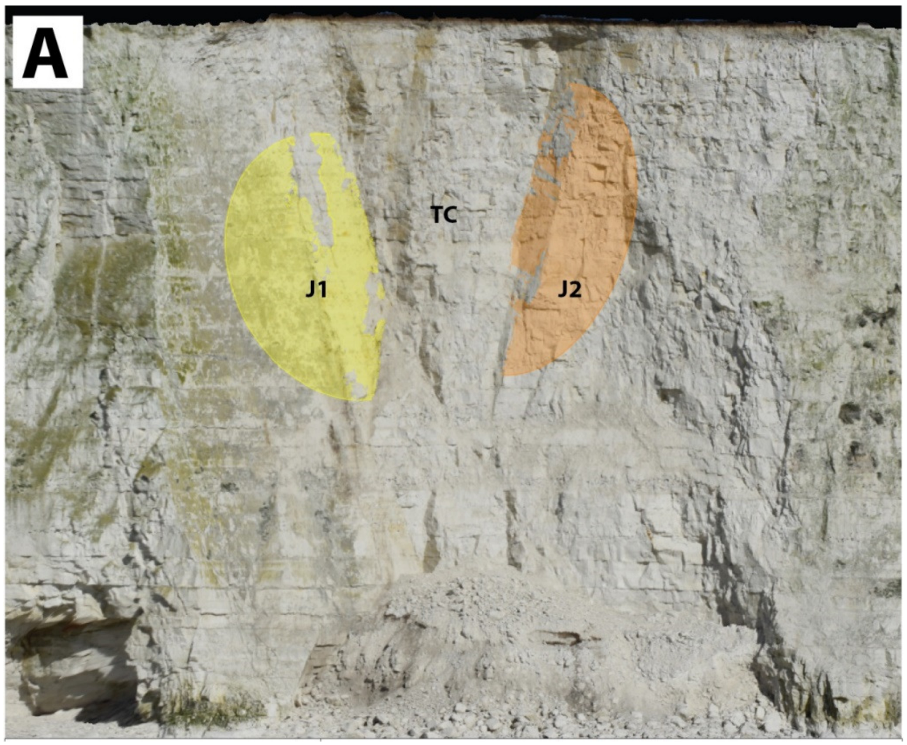

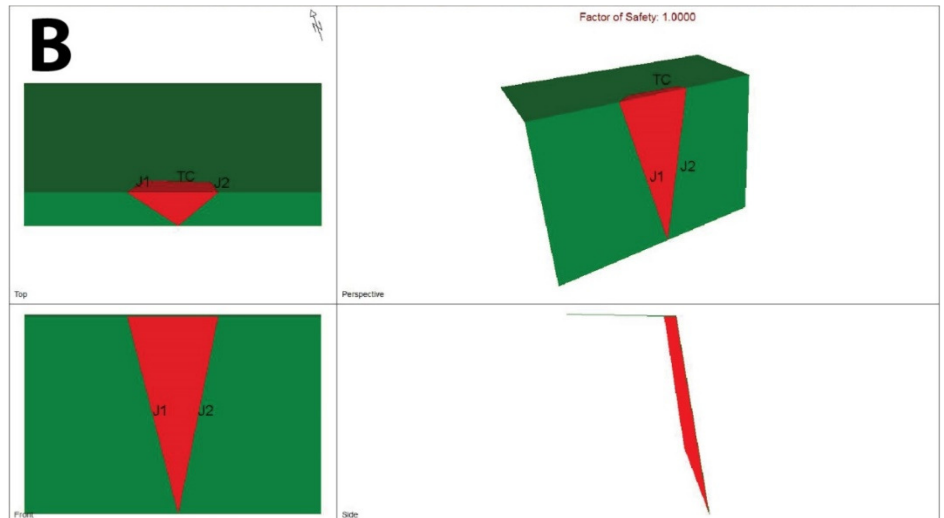

C

Slope (Cliff face)		Tension Crack (TC)		Joints			
Dip	80.43°	Dip	81.67°	Joint 1 (J1)		Joint 2 (J2)	
Dip direction	200.2°	Dip direction	201.57°	Dip	74.07°	Dip	75.27°
Height	41.83m	Trace length	4.41m	Dip direction	165.51°	Dip direction	253.43°
				Waviness	0°	Waviness	0°
Upper face							
Dip	1°			Shear strength model	Mohr-Coulomb	Shear strength model	Mohr-Coulomb
Dip direction	200.2°						
				cohesion (c)	23.044 kPa	cohesion (c)	23.044 kPa
Unit weight	16 kN/m^3			angle of friction (ϕ)	38°	angle of friction (ϕ)	38°

Photogrammetry – discontinuity analysis

Wedge failure – analysis (Swedge)

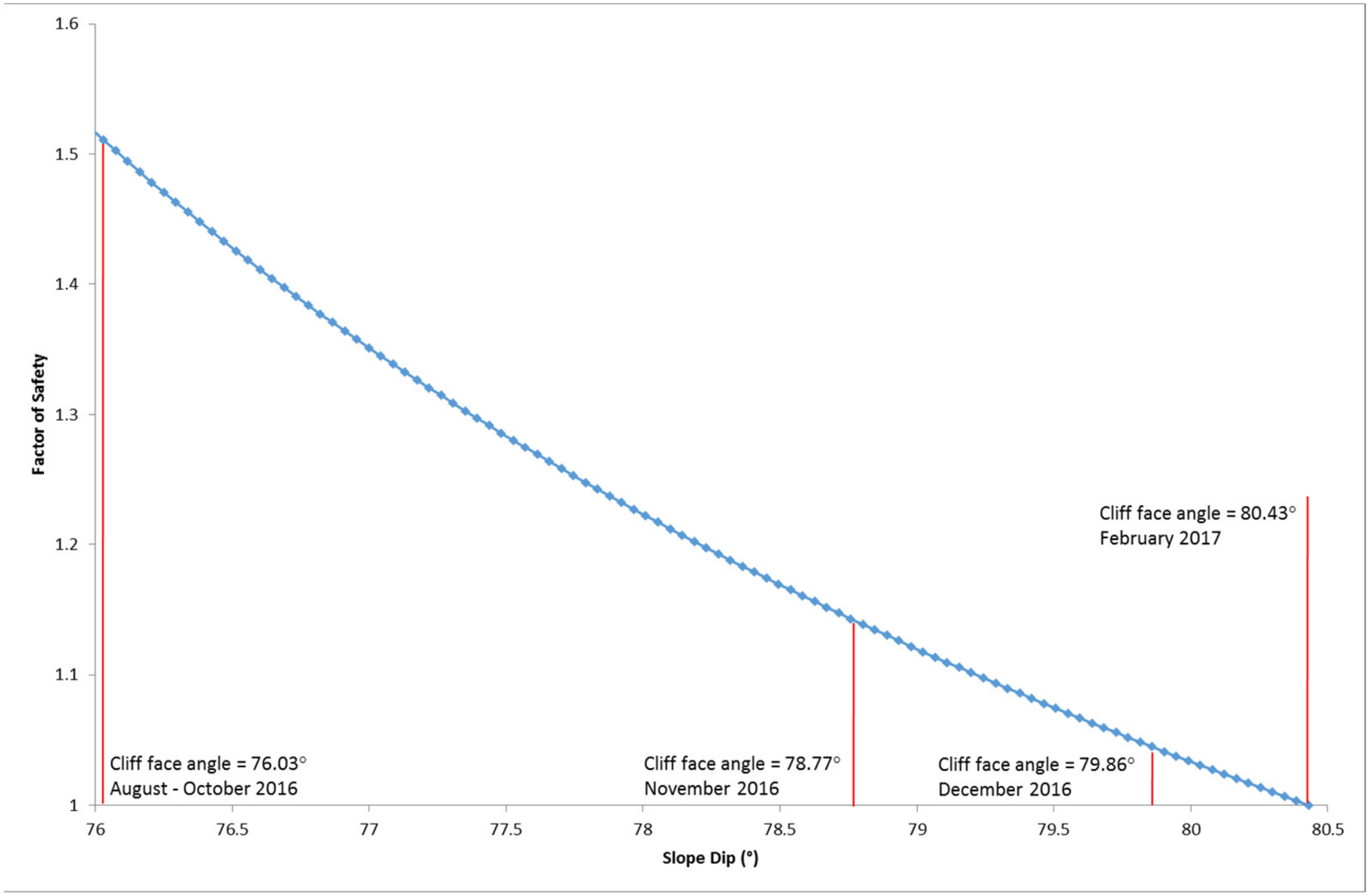

JACOBS

Photogrammetry – discontinuity analysis

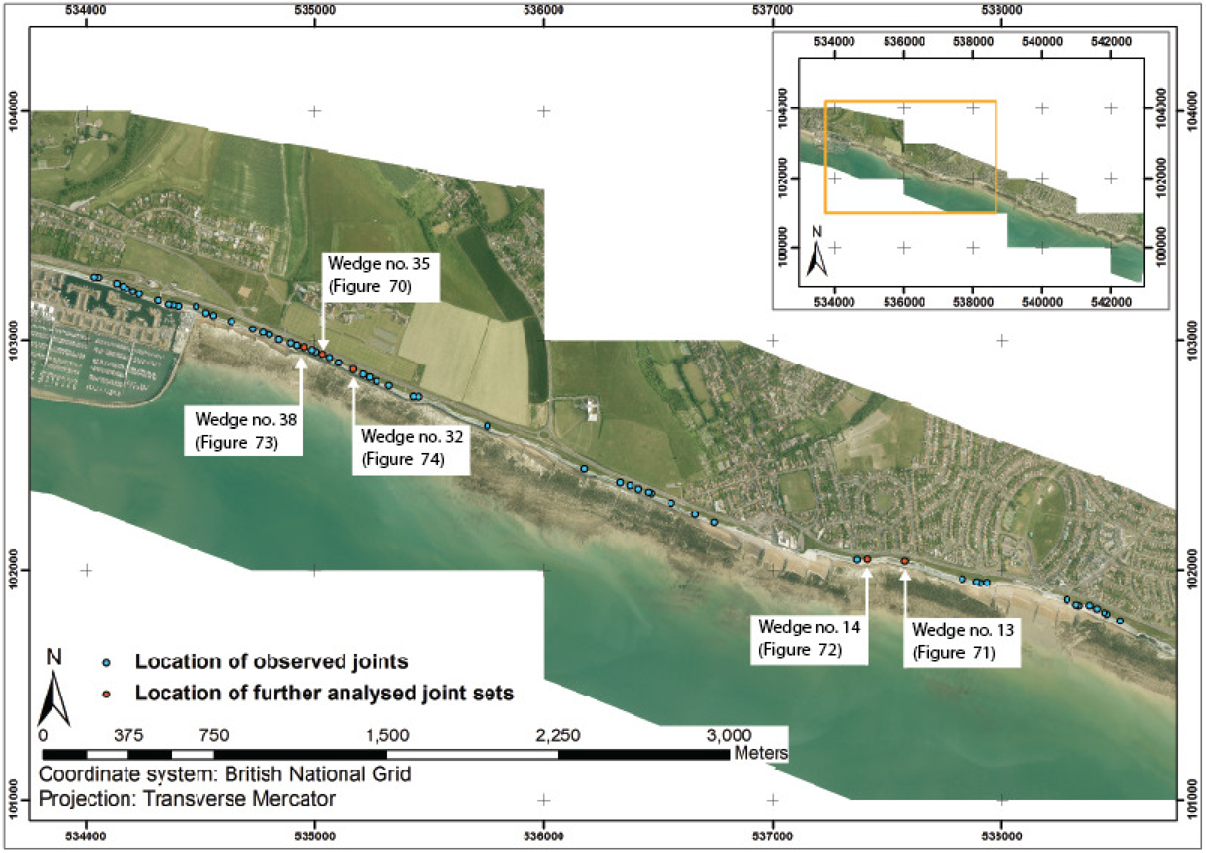

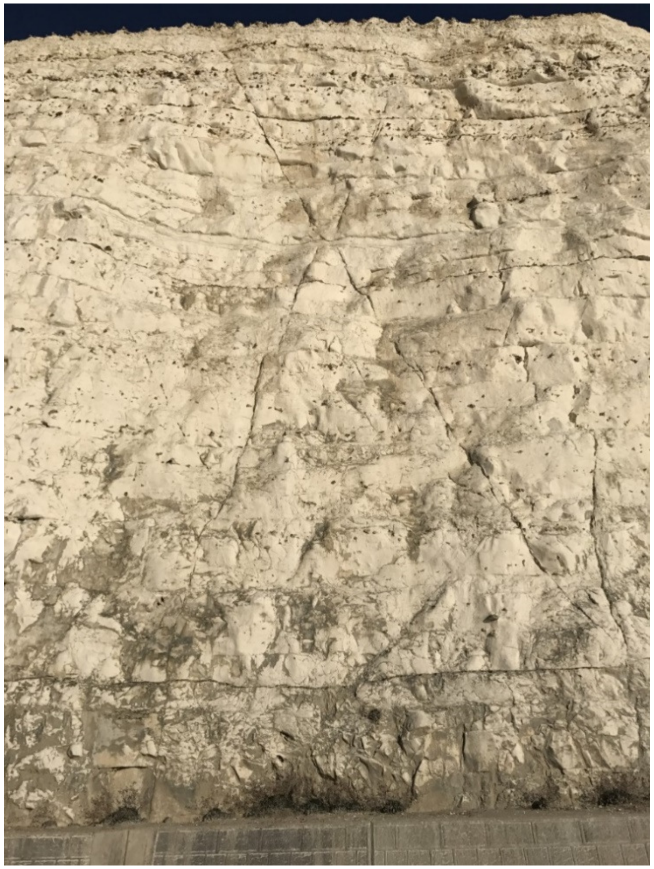

JACOBS

Photogrammetry – discontinuity analysis

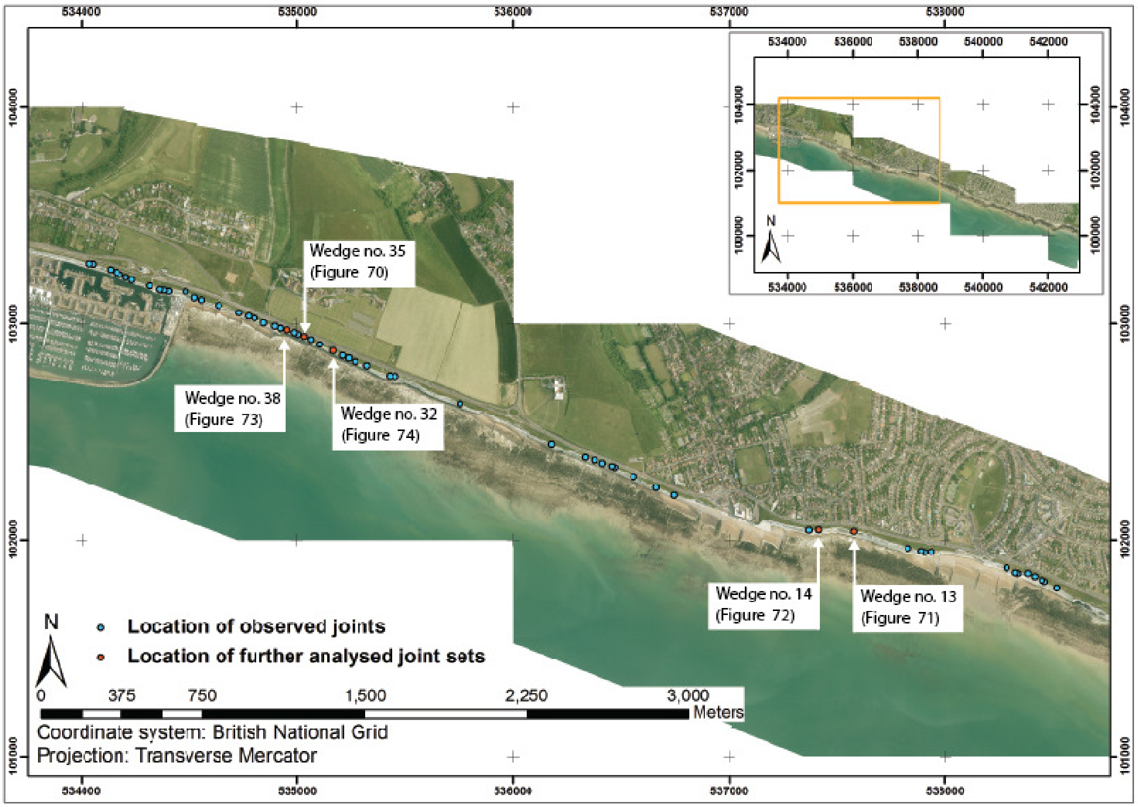

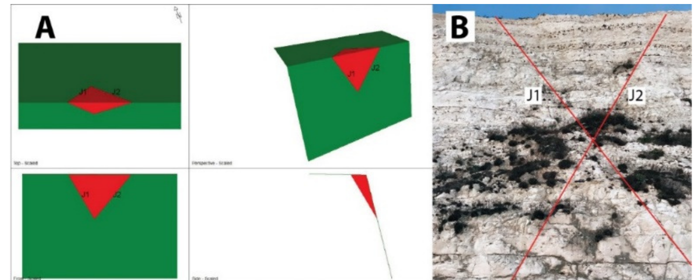

	Cohesion (kPa)			
	c' (9.45)*	c' (10.24)*	c' (27.25)*	c peak (80.00)**
Factor of safety	1.239	1.299	2.607	6.664

JACOBS

Photogrammetry – overview

Developed a reliable UAV photogrammetry methodology for acquiring high resolution datasets for monitoring sea cliffs

Results have comparable accuracy to currently deployed TLS/ALS

Software platforms enable processing of large datasets into manageable formats – enables subsequent data analysis (e.g. surface change, kinematics)

Statistical analysis enabled the first probabilistic negative power law model of cliff recession constrained by environmental conditions to be developed

October 15, 2019

JACOBS

www.jacobs.com | worldwide